nature reviews earth & environment

https://doi.org/10.1038/s43017-022-00381-x

Review article

Check for updates

Trends and variability in the ocean carbon sink

Nicolas Gruber[1] ✉, Dorothee C. E. Bakker[2], Tim DeVries[3,4], Luke Gregor[1], Judith Hauck[5], Peter Landschützer[6,7], Galen A. McKinley[8,9] & Jens Daniel Müller[1]

Abstract

The ocean has absorbed 25 ± 2% of the total anthropogenic CO_2 emissions from the early 1960s to the late 2010s, with rates more than tripling over this period and with a mean uptake of −2.7 ± 0.3 Pg C $year^{-1}$ for the period 1990 through 2019. This growth of the ocean sink matches expectations based on the increase in atmospheric CO_2, but research has shown that the sink is more variable than long assumed. In this Review, we discuss trends and variations in the ocean carbon sink. The sink stagnated during the 1990s with rates hovering around −2 Pg C $year^{-1}$, but strengthened again after approximately 2000, taking up around −3 Pg C $year^{-1}$ for 2010–2019. The most conspicuous changes in uptake occurred in the high latitudes, especially the Southern Ocean. These variations are caused by changes in weather and climate, but a volcanic eruption-induced reduction in the atmospheric CO_2 growth rate and the associated global cooling contributed as well. Understanding the variability of the ocean carbon sink is crucial for policy making and projecting its future evolution, especially in the context of the UN Framework Convention on Climate Change stocktaking activities and the deployment of CO_2 removal methods. This goal will require a global-level effort to sustain and expand the current observational networks and to better integrate these observations with models.

Sections

[1]Environmental Physics, Institute of Biogeochemistry and Pollutant Dynamics, ETH Zurich, Zürich, Switzerland. [2]Centre for Ocean and Atmospheric Sciences, School of Environmental Sciences, University of East Anglia, Norwich, UK. [3]Department of Geography, University of California, Santa Barbara, CA, USA. [4]Earth Research Institute, University of California, Santa Barbara, CA, USA. [5]Alfred-Wegener-Institut, Helmholtz-Zentrum für Polar und Meeresforschung, Bremerhaven, Germany. [6]The Ocean in the Earth System, Max Planck Institute for Meteorology, Hamburg, Germany. [7]Department Research, Flanders Marine Institute (VLIZ), Ostend, Belgium. [8]Department of Earth and Environmental Sciences, Columbia University, New York, NY, USA. [9]Lamont Doherty Earth Observatory, Palisades, NY, USA. ✉e-mail: nicolas.gruber@env.ethz.ch

Key points

- The long-term trend in the ocean carbon sink since the early 1960s was primarily driven by the increasing uptake of anthropogenic CO_2. Although the ocean is expected to have lost a few petagrams of natural CO_2 to the atmosphere in response to ocean warming, this loss cannot be quantified conclusively with observations.
- The oceanic uptake of anthropogenic CO_2 scaled proportionally with the increase in atmospheric CO_2 between the early 1960s and late 2010s, as expected given the quasi-exponential growth of atmospheric CO_2 during this period.
- The average ocean uptake rate of -2.7 ± 0.3 Pg C year^{-1} for the period 1990 through 2019 is commensurate with a sensitivity β of 1.4 ± 0.1 Pg C per ppm atmospheric CO_2, suggesting a trend in the uptake of -0.4 ± 0.1 Pg C year^{-1} per decade.
- The annual mean ocean carbon sink varies by about ±20% around this trend, primarily caused by changes in the sources and sinks of natural CO_2, with a lesser role for variations in atmospheric CO_2 growth rates impacting the uptake of anthropogenic CO_2.
- The net oceanic uptake rate of CO_2 will likely decrease in the future owing to several converging trends: reduced emissions of CO_2 leading to reduced atmospheric CO_2 growth rates in response to climate policy; reduced storage capacity owing to continuing ocean acidification; and enhanced outgassing of natural CO_2 owing to ocean warming and changes in ocean circulation and biology.

Introduction

Throughout the Anthropocene, the ocean has been the largest and most persistent sink for the anthropogenic CO_2 emitted into the atmosphere by the burning of fossil fuels, cement production and land use change[1–4]. This importance was recognized already by the late nineteenth century[5,6], with the chemist Arrhenius estimating that about 83% of the emitted anthropogenic CO_2 would be taken up by the ocean[7]. Therefore, Arrhenius concluded that no noticeable global warming should be expected from the emissions of anthropogenic CO_2, as the uptake by the ocean leaves only a small fraction of the emissions accumulating in the atmosphere. Although his estimate of the long-term capacity of ocean uptake was accurate[8,9], Arrhenius was not aware that it takes thousands of years for the ocean to fully realize this capacity and not decades as he implicitly assumed[6]. Arrhenius' incorrect view was widely shared, so that the scientific community was oblivious to the growing threat from the CO_2 emissions that were increasing by several per cent per year for most of the early twentieth century[10]. Revelle and Suess realized this mistake in 1957 (ref. 11). Thereafter, the perspective of the scientific community on the issue of human-induced climate change shifted rapidly[12,13], especially after Keeling confirmed in 1960 that atmospheric CO_2 was increasing much more rapidly than implied by Arrhenius[14].

Much of the global ocean carbon cycle research since Revelle and Suess' discovery has focused on quantifying the fraction of the CO_2 emissions taken up by the ocean, and to understand the processes that limit this uptake, preventing the ocean from reaching the huge capacity of more than 80% that Arrhenius had identified. A crucial step to address this question was the conceptualization of the net exchange of CO_2 across the air–sea interface and the change in the stock of dissolved inorganic carbon (DIC) to consist of two components: anthropogenic CO_2 and natural CO_2 (Box 1). The anthropogenic CO_2 component (C_{ant}), previously often referred to as excess CO_2 (ref. 15), can be considered the perturbation component, as it is solely a consequence of the anthropogenic increase in atmospheric CO_2. The natural CO_2 component (C_{nat}) of the flux is associated with the preindustrial pool of DIC in the ocean (in the order of 37,000 Pg C (1 Pg = 10^{15} g))[16] and is involved in air–sea gas exchange, uptake and release by the biological pumps, interactions with and loss to the sediments, and input by rivers (Box 1).

Under the assumption of a steady-state ocean, which is supported by the relative constancy of climate and atmospheric CO_2 for centuries prior to the onset of the industrial revolution (approximately 1800)[17], the oceanic pool of natural CO_2 remains constant and the fluxes of natural CO_2 are globally balanced. This assumption permitted researchers already in the 1970s to use models and observations to determine the oceanic uptake of anthropogenic CO_2 (refs. 18–20), with subsequent work refining the methods and improving the database[2,4,15,21,22].

However, it has become increasingly clear since the 2000s that the natural carbon fluxes of the ocean are changing, and that the ocean sink for carbon is more variable[23–32]. The natural CO_2 pool is in fact highly mobile, responding to changes in physical forcing from the atmosphere through changes in winds and in the fluxes of heat and freshwater, inducing changes in ocean circulation, temperature, salinity and ocean biology[9]. Moreover, the anthropogenic CO_2 pool is more changeable than previously thought, responding to changes in the atmospheric CO_2 growth rate or changes in ocean circulation[33].

In this Review, we assess what is currently known about the ocean sink for CO_2, and how it has responded to the rising CO_2 emissions in recent decades, relying primarily on ocean observations. We describe the variability of this sink and its drivers, which are debated. Finally, we highlight the need for increased observational capacity to support long-term decision making, especially for the use of oceanic CO_2 removal (negative emission) approaches.

Ocean carbon sink trends

Since the late 1950s, the ocean has taken up a net 25 ± 2% of the total anthropogenic CO_2 emissions[1]. This fractional uptake has remained relatively constant through time, meaning that the ocean sink tripled over these six decades, increasing from about −0.9 Pg C year^{-1} in the early 1960s to about −3 Pg C year^{-1} in 2020 (refs. 1,25) (note that the geophysical convention of fluxes being are considered positive here, so that an uptake of CO_2 is negative). This increasing ocean carbon sink is an ecosystem service that amounts to about €2 trillion worth of emission reductions per year if valued at a typical marginal abatement cost compatible with a 1.5 °C target of €200 per ton of CO_2 (ref. 34). Together with the large ocean uptake of the excess heat generated from rising atmospheric CO_2 (ref. 35), the ocean has moderated the climate change experienced so far[36,37]. This section reviews how this ocean carbon sink has been determined and what drives this long-term trend.

Response to rising atmospheric CO_2

The primary driver causing a long-term (more than a decade) change in the ocean's inventory of DIC is the rise in atmospheric CO_2, driving a flux of anthropogenic CO_2 across the air–sea interface and then from the surface ocean to depth (Box 1). The rate limiting step for the uptake of anthropogenic CO_2 by the ocean is the transport from the surface to deeper layers[38], as it takes decades to centuries for waters to circulate from the surface to the deeper ocean and back again[39,40].

Box 1

Key concepts in ocean carbon sink investigations

Natural versus anthropogenic CO_2

A key concept aiding the interpretation of the ocean carbon sink has been the separation of the air–sea CO_2 fluxes and the changes in the ocean interior storage of dissolved inorganic carbon (DIC) into natural and anthropogenic CO_2 components[38]. The natural CO_2 component (C_{nat}) is the part of the ocean's DIC pool that existed in preindustrial times. This pool is involved in many processes, namely air–sea gas exchange, uptake and release by the biological pumps, interactions with and loss to the sediments, and input by rivers (see the figure, part **a**). The anthropogenic CO_2 component (C_{ant}) represents the perturbation to the DIC pool, driven by the anthropogenically driven increases in atmospheric CO_2. It is substantially smaller than the natural DIC pool (see the figure, part **b**).

An important assumption that has simplified the analysis is that the C_{ant} does not interact with the C_{nat} (ref. 38). Therefore, the only processes of importance for anthropogenic CO_2 are the uptake from the atmosphere via air–sea gas exchange and the subsequent transport to depth (see the figure, part **a**). The assumption about the lack of interaction between the two pools is generally well met, but there are some exceptions. For example, the acidification induced by the oceanic accumulation of anthropogenic CO_2 can affect ocean biology[157] and also has been shown to modify the flux of natural CO_2 (refs. 158,159).

The steady-state ocean

The second key concept is steady state, which is reached if climate forcing remains constant for long enough for ocean circulation and ocean biology to become unchanging with time. In this situation, natural CO_2 fluxes across the air–sea interface balance to zero on a global scale[104], with the exception of steady-state outgassing of river-derived CO_2 (ref. 105). Biological fluxes are also balanced over the annual cycle. The only variations in time come from the steady-state uptake of anthropogenic CO_2 (see the figure, parts **c,e**). If climate is permitted to vary, leading to a non-steady-state situation, both natural and anthropogenic CO_2 components are affected, leading to additional fluxes and changes in storage (see the figure, parts **d,f**). The non-steady-state component of natural CO_2 emerges from a situation where climate is varying, but where atmospheric CO_2 is kept at its preindustrial level (see the figure, part **d**). The difference between this situation and one where atmospheric CO_2 is permitted to increase gives the non-steady-state component of anthropogenic CO_2 (see the figure, part **f**). DIC_{tot}, total dissolved inorganic carbon.

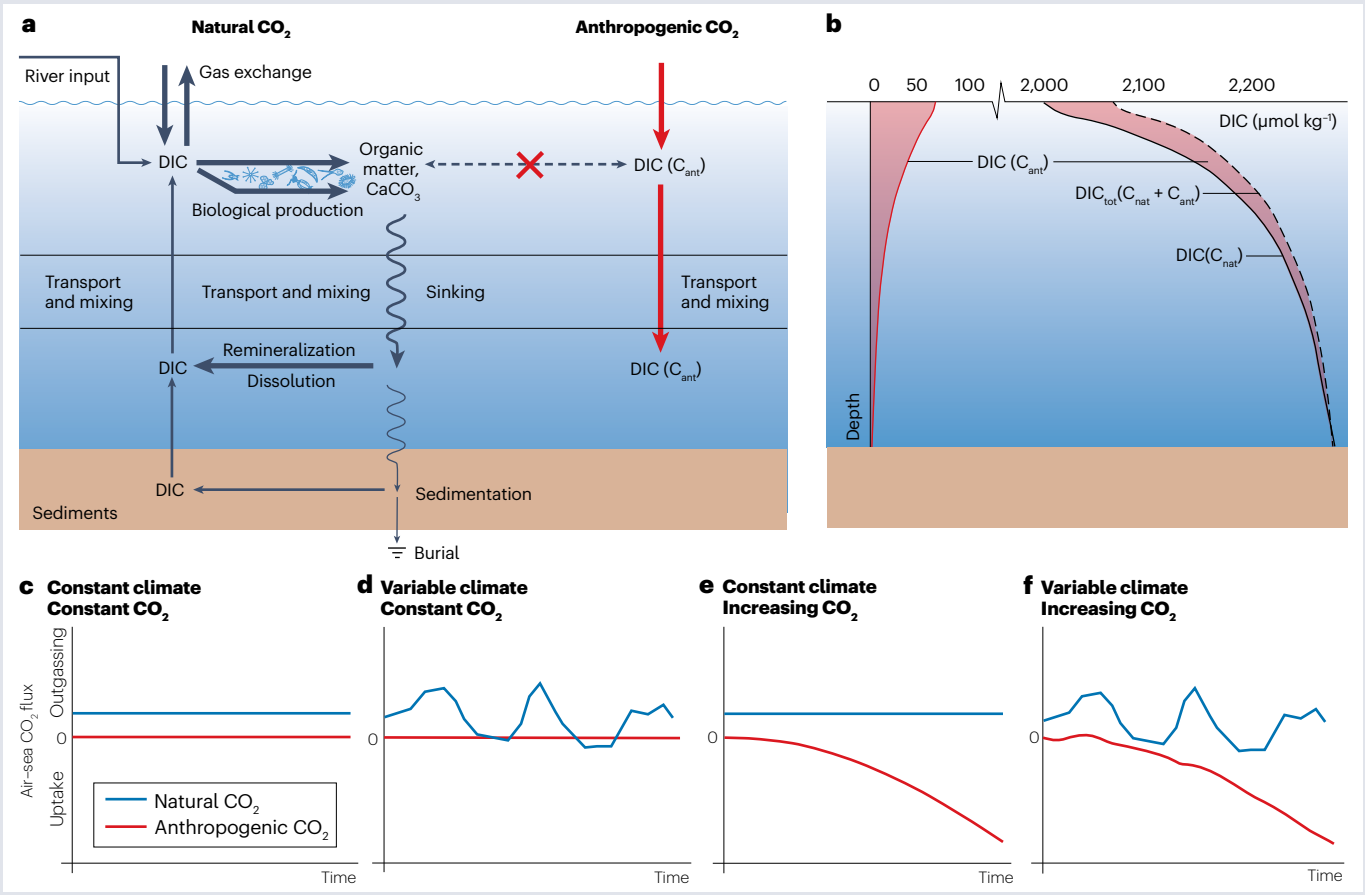

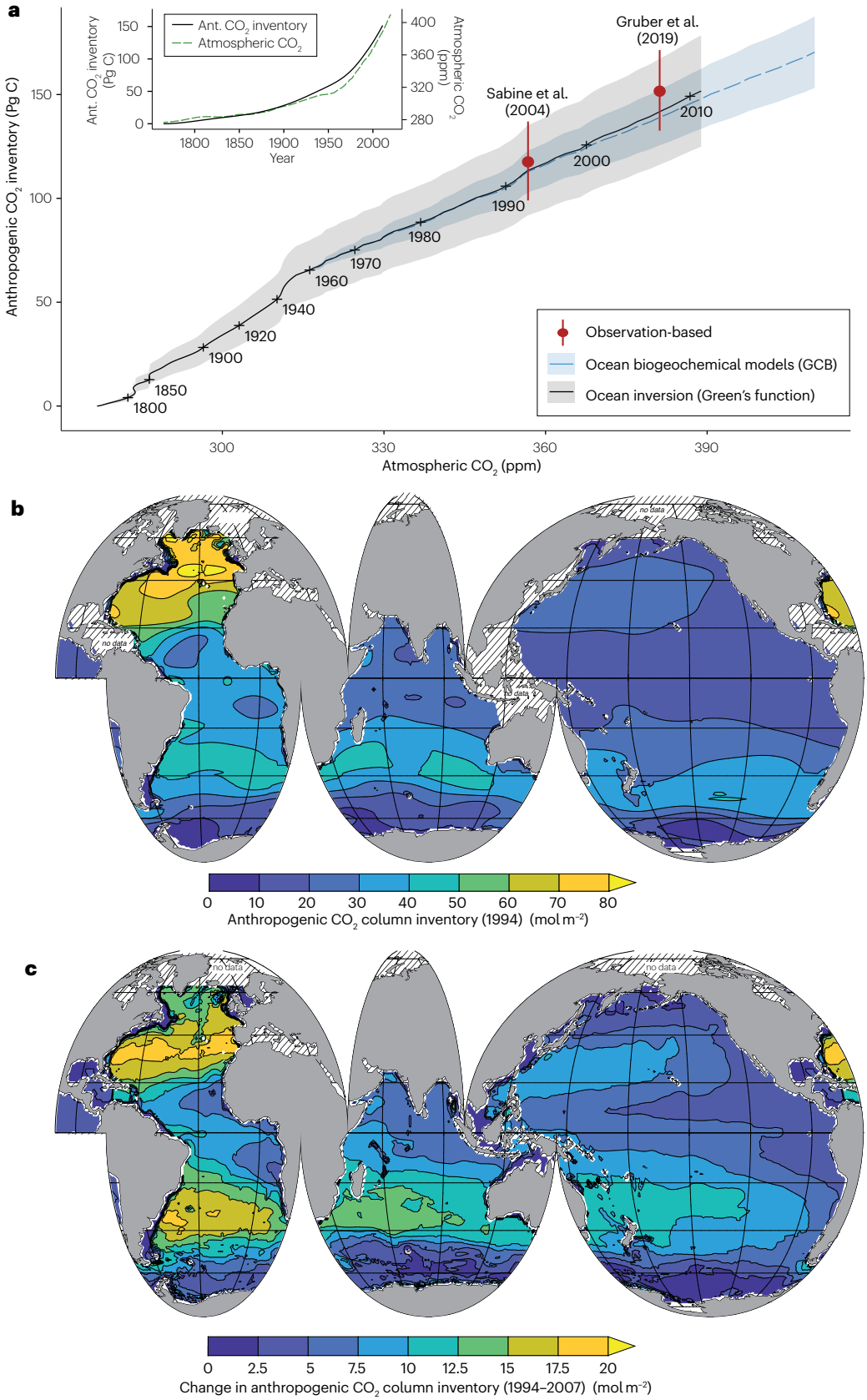
a
Anthropogenic CO2 inventory (Pg C)
Atmospheric CO2 (ppm)
Ant. CO2 inventory (Pg C)
Atmospheric CO2 (ppm)
Year
Ant. CO2 inventory
Atmospheric CO2
Gruber et al. (2019)
Sabine et al. (2004)
1800
1850
1900
1920
1940
1960
1970
1980
1990
2000
2010
Observation-based
Ocean biogeochemical models (GCB)
Ocean inversion (Green's function)
b
no data
0 10 20 30 40 50 60 70 80
Anthropogenic CO2 column inventory (1994) (mol m-2)
c
no data
0 2.5 5 7.5 10 12.5 15 17.5 20
Change in anthropogenic CO2 column inventory (1994–2007) (mol m-2)

Fig. 1 | Ocean uptake and storage of anthropogenic CO_2. a, Temporal progression of the total ocean inventory of anthropogenic CO_2 as a function of the atmospheric CO_2 content. Results are from an ocean inverse model[3] (black line and grey shaded band indicating uncertainty) spanning the period from 1765 until 2010, the ocean biogeochemical model results used in the Global Carbon Budget (GCB)[25] (blue dashed line for the mean and blue shaded band representing the standard deviation) and two observation-based estimates of the ocean interior accumulation of anthropogenic CO_2 (refs. 2,4) for 1994 and 2007. Inset: the time history of atmospheric CO_2 and the ocean inventory of anthropogenic CO_2 (ref. 3). The bands represent the cumulative uncertainty from the start of the respective estimate. The nearly linear scaling of the oceanic inventory with atmospheric CO_2 is particularly evident after 1959. The ocean biogeochemical model results shown here include also the non-steady-state component of natural CO_2 (climate variability). **b**, Column inventory of anthropogenic CO_2 (moles per square metre) for the year 1994 estimated using the ΔC^* back-calculation method[2]. Strong regional patterning of the accumulation of anthropogenic CO_2 in the ocean was driven by regional differences in ocean circulation and mixing. **c**, Change in the water column inventory between 1994 and 2007 estimated by the eMLR(C*) method[4]. In panels **b** and **c**, the hatching indicates regions that were not mapped. eMLR, extended multiple linear regression.

By contrast, CO_2 gas exchange across the air–sea interface is comparably fast (e-folding time scale of less than a year[9,41]), so that the CO_2 concentration of the surface ocean follows the atmospheric perturbation relatively closely[42–44], with the magnitude of increase determined by the surface ocean's buffer factor (also called the Revelle factor)[9,45,46]. The two processes of air–sea exchange and the surface to deep transport of CO_2 respond approximately linearly to changes in atmospheric CO_2. However, there is some moderate non-linearity owing to the ocean's decreasing buffering capacity due to ocean acidification (a decrease of about 10% since preindustrial times[47]) that needs to be taken into account as well[48,49].

When a (near-)linear system such as the ocean uptake of anthropogenic CO_2 (C_{ant}) is forced exponentially with a fixed growth rate (as is the case for atmospheric CO_2 since approximately 1970) (Fig. 1a), all components of the system will increase proportionally after an initial adjustment (which is about a decade[50]). This proportionality implies a linear scaling between the forcing (atmospheric CO_2) and the response (ocean accumulation of anthropogenic CO_2), which is confirmed by results from observations[2,4], ocean inverse models[3] and forward simulations with ocean biogeochemical models[25,51] (Fig. 1a). The slope of this relationship (Fig. 1a, lines with shading) represents the carbon concentration feedback of the ocean[52,53] and is described as the sensitivity $\beta = \partial C_{ant}/\partial \Delta CO_2{}^a$, where $\Delta CO_2{}^a$ is the change in atmospheric CO_2 since preindustrial times. The exact value of β depends on the forcing history and, especially, past atmospheric growth rate. An emergent property of this relationship is that during periods of exponential growth in atmospheric CO_2, it directly determines the global oceanic uptake flux of anthropogenic CO_2 ($F_{ant}(t)$) from the growth rate of atmospheric CO_2: $dC_{ant}/dt = -F_{ant}(t) = \beta \cdot d\Delta CO_2{}^a/dt$, where the negative sign in front of F_{ant} reflects the convention of ocean uptake being negative.

This simple scaling relationship does not apply once the atmospheric CO_2 growth begins to deviate substantially from an exponential, as is expected if emissions start to stabilize and decrease in response to global efforts to curb climate change[54]. In such cases, more complete theories building on deconvolution concepts such as pulse response functions[3,55] or transit time distributions[56–58] are much better suited to describe the oceanic uptake of anthropogenic CO_2 (ref. 59). Nevertheless, the high CO_2 concentration in the atmosphere would still be the main driving force for the many centuries it takes to equilibrate the entire ocean with the atmospheric perturbation[60].

Cumulative oceanic uptake

The tight relationship between the ocean uptake for anthropogenic CO_2 and the growth in atmospheric CO_2 was recognized by the 1970s (refs. 18,61,62). However, until the mid-1980s, high-quality measurements of oceanic DIC were extremely scarce[63], making it impossible to constrain this relationship with observations. As the number of reliable DIC measurements increased, methods to identify the anthropogenic CO_2 signal within the substantial background variability of DIC emerged[19,20]. As the data were typically available only from a one-time survey, back-calculation approaches were used that implicitly assume a steady-state ocean. In such approaches, the DIC concentration in a water parcel in the ocean's interior is traced back to its origin at the surface, correcting along the way for the biological changes that incurred along this journey from the surface to depth[15,21]. Refinement of the initial approaches led to the ΔC^* method[64,65], which is the most widely used back-calculation method to identify the total amount of anthropogenic CO_2 that has accumulated in the ocean since preindustrial times[21]. A crucial enabling development for the identification of the relatively small anthropogenic CO_2 signal (see also Box 1) was the introduction of common measurement methodologies[66] and certified reference materials[67,68] that permitted the collation of DIC measurements taken years apart and measured by different laboratories around the world into an internally coherent data set[69].

The application of the ΔC^* approach to the data collected by the Joint Global Ocean Flux Study (JGOFS)/World Ocean Circulation Experiment (WOCE) programmes in the mid-1980s to mid-1990s led to the first global data-based estimate of the accumulation of anthropogenic CO_2 (ref. 2). This approach yielded a total anthropogenic CO_2 inventory for the nominal year 1994 of 118 ± 19 Pg C (Fig. 1a), that is, reflecting the time-integrated ocean uptake since approximately 1800. The map in Fig. 1b shows the well-established spatial variations in the vertically integrated amount of anthropogenic CO_2 (refs. 38,70–72). Strong accumulation in the North Atlantic contrasts with regions of relatively low accumulation such as the Tropical Pacific and the polar Southern Ocean. One of the most conspicuous features of the spatial variation is the band of high accumulation north of the Southern Ocean between about 30° S and 40° S. These basin-scale differences are a direct consequence of the regional effectiveness with which anthropogenic CO_2 is transported from the surface downward into the ocean's interior[70,72–74]. The Ocean Inversion Project used such knowledge about the surface to depth transport in the form of impulse response functions, to estimate how much uptake of anthropogenic CO_2 is required in order to match the reconstructed distribution of anthropogenic CO_2 in 1994. This estimate yielded an uptake flux of −2.2 ± 0.25 Pg C $year^{-1}$ for the nominal year 1995 (ref. 72).

This inventory also provided the first observation-based estimate of the sensitivity β of 1.47 ± 0.24 Pg C per ppm CO_2, representing the time period 1800–1994 (see Supplementary Table 1). These results confirmed many prior estimates that so far had relied on models[18,38,71], indirect constraints such as the changes in atmospheric oxygen[75] or budgets of the stable isotope of carbon (^{13}C)[76–78].

Decadal trends in uptake

Linear β-scaling can be used to provide a first estimate of the further evolution of the oceanic sink. Given the observed trend in the atmospheric CO_2 growth rate of 0.3 ppm year^{-1} decade^{-1} between 1994 and 2007 and the inferred sensitivity β of 1.47 ± 0.24 Pg C per ppm CO_2, one would expect the steady-state ocean sink for anthropogenic CO_2 to increase (become more negative) by about −0.4 Pg C year^{-1} decade^{-1} over this period, yielding an uptake in 2007 of the order of −2.6 Pg C year^{-1}. Forward and inverse models[3,25,70,79] have been used to assess this trend prediction (Fig. 1a), but the ultimate evidence has to come from direct documentation of the increase in the ocean's DIC pool.

Direct documentation of decadal trends in anthropogenic CO_2 uptake is not straightforward, as shorter-term variations in the natural carbon pool tend to mask the slower but steadier increase in anthropogenic CO_2. This problem can be overcome for regularly sampled time series[43,80,81], but only a few sites have sufficient observations to distinguish the anthropogenic trend from the natural variability. In most cases, the sampling rate is once per decade, as is the case for the GO-SHIP Global Repeat Hydrography Program[82], for example. These data suffer acutely from an overprint of short-term variability in the natural carbon cycle, typically leading to a very noisy pattern of change that is difficult to interpret[83].

The introduction of the extended multiple linear regression (eMLR) approach[84] enabled the change in anthropogenic CO_2 to be mostly isolated[85,86]. This method is the most widely used approach for detecting and quantifying changes in the anthropogenic CO_2 in the interior ocean based on repeat hydrography cruises[83,87–89]. Compared with the ΔC* approach, the eMLR approach captures both the steady-state and the non-steady-state accumulation of anthropogenic CO_2, although with limited accuracy when reconstructing the non-steady-state component[90].

A modified version of the eMLR method (eMLR(C*) method[90]) was used to estimate the change in anthropogenic CO_2 (ΔC_{ant}) globally[4], using DIC and other biogeochemical data from the JGOFS/WOCE survey for the 1990s and comparing them with the measurements from the 2000s obtained during the first round of the GO-SHIP Repeat Hydrography Program[82] (Fig. 1c). Global ocean carbon storage was estimated[4] to increase by 34 ± 4 Pg C between 1994 and 2007, bringing the total inventory for anthropogenic CO_2 for 2007 to 154 ± 19 Pg C (Fig. 1a). This increase in storage corresponds to a mean ocean uptake flux of anthropogenic CO_2 of −2.6 ± 0.3 Pg year^{-1} over the 1994–2007 period, corroborating the simple scaling prediction. It also suggests a sensitivity β of 1.39 ± 0.16 Pg C per ppm CO_2, which is statistically indistinguishable from that estimated from the anthropogenic CO_2 inventory in 1994 (1.47 ± 0.24 Pg C per ppm CO_2; see Supplementary Table 1). This lack of a difference provides strong support for the steady-state assumption.

Given this steady state, the ocean interior estimate for 1994–2007 can be scaled to each decade over the past 30 years using β, yielding −2.1 Pg C year^{-1} for 1990–1999, −2.6 Pg C year^{-1} for the subsequent decade and −3.3 Pg C year^{-1} for 2010–2019 (Table 1). Models suggest a smaller sensitivity β, lower mean uptake and smaller decadal trends (Table 1; see Supplementary Table 1). However, many of the differences are not statistically significant, confirming that the ocean acts as a strong and increasing sink for anthropogenic CO_2. Overall, the steady-state assumption is useful for determining the multidecadal oceanic uptake of anthropogenic CO_2. However, this assumption does not hold as well when analysing shorter-term variations or spatial variations.

Non-steady-state uptake

A more detailed analysis of the spatial variations in the ocean interior accumulation of anthropogenic CO_2 highlights the limits of the steady-state assumption (Fig. 1b,c). To first order, the increase in anthropogenic CO_2 is proportional to how much anthropogenic CO_2 was present at the beginning[4,42,91]. The proportionality can be estimated using the β approach, yielding a value of 0.28 ± 0.02 for the inventory in 1994 and the change in inventory[4] between 1994 and 2007 (similar approaches using a transit time distribution approach[57] yield comparable results). Thus, differences in the scaled spatial distribution of C_{ant} (1994) (Fig. 1b) and ΔC_{ant} (2007–1994) (Fig. 1c) suggest a non-steady-state contribution. Although the uncertainties in the two reconstructions are substantial, they suggest a shift in the accumulation of anthropogenic CO_2 from the North Atlantic to the South Atlantic, potentially related to decadal shifts in the overturning circulation[92]. This pattern confirms the presence of substantial decadal variability in the ocean carbon cycle

Table 1 | Ocean CO_2 uptake from 1990 to 2019

Method	Components	1990–1999 (Pg C year^{-1})	2000–2009 (Pg C year^{-1})	2010–2019 (Pg C year^{-1})	Ref.
Atmospheric CO_2					
Change in atmospheric CO_2 (ppm)		15.0	18.7	23.6	155
Ocean CO_2 uptake					
Change in interior accumulation of anthropogenic CO_2 [a]	$F_{ant}^{ss}+F_{ant}^{ns}$	−2.1±0.2	−2.6±0.3	−3.3±0.3	4
Ocean inverse model (Green's function)	F_{ant}^{ss}	−2.0±0.6	−2.3±0.6	NA	3
Ocean inverse model (adjoint method)	F_{ant}^{ss}	−2.2±0.1	−2.5±0.1	−2.9±0.2	136
Ocean inverse model (adjoint method)[b]	$F_{ant}^{ss}+F_{nat}^{ns}$	−2.0±0.1	−2.3±0.1	−2.7±0.2	136
Ocean forward models	$F_{ant}^{ss}+F_{ant}^{ns}+F_{nat}^{ns}$	−2.0±0.2	−2.1±0.3	−2.5±0.3	25
Surface pCO_2 products[c]	$F_{ant}^{ss}+F_{ant}^{ns}+F_{nat}^{ns}$	−2.1±0.4	−2.3±0.2	−3.1±0.2	103

F_{ant}^{ns}, non-steady-state uptake component of anthropogenic CO_2 (part driven by variations in ocean circulation and other physical drivers); F_{ant}^{ss}, steady-state uptake flux component of anthropogenic CO_2 (part driven solely by the increase in atmospheric CO_2); F_{nat}^{ns}, non-steady-state exchange component of natural CO_2 (part driven by variations in ocean circulation and other physical drivers) (see Box 1); NA, not available; pCO_2, partial pressure of CO_2. [a]Scaled using sensitivity β=1.39 ± 0.16 Pg C per ppm CO_2 and the change in atmospheric CO_2 indicated in the first row. [b]Non-steady-state component is only due to variability in sea-surface temperature. [c]Adjusted for the steady-state outgassing of river-derived CO_2.

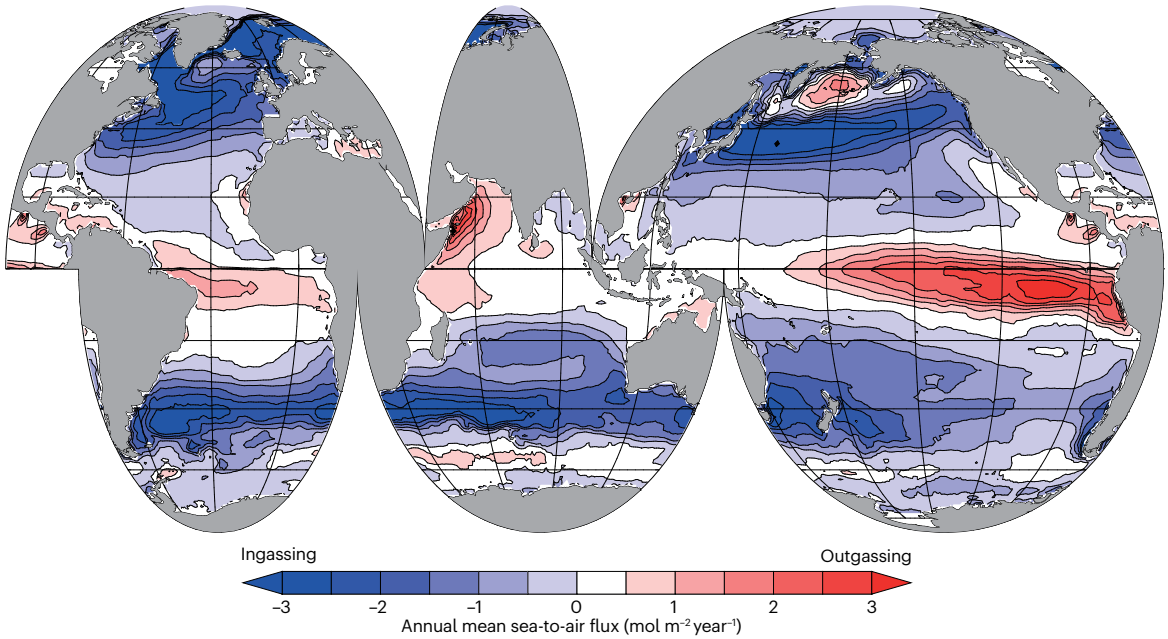

Fig. 2 | Climatological mean sea-to-air CO_2 flux. Multi-product mean estimate based on the six ocean partial pressure of CO_2 (pCO_2)-based estimates contained in the SeaFlux product[103]. The mean for the period 1990 through 2020 is depicted, representing the sum of natural, anthropogenic and steady-state riverine flux components for the nominal year of 2005. The global ocean is characterized by regions of strong sources and sinks of CO_2, reflecting primarily the exchange of natural CO_2 across the air–sea interface. This flux is regionally modified by the uptake flux of anthropogenic CO_2. The latter integrates globally to an uptake flux of about 2.6 Pg C $year^{-1}$ for this nominal year. The total CO_2 flux also includes an outgassing flux of about 0.65 ± 0.30 Pg C $year^{-1}$, reflecting the steady-state outgassing of natural CO_2 associated with the imbalance between river input and burial[105].

identified previously along basin-wide hydrographic sections that had been occupied multiple times[83,89]. However, the decadal nature of the repeat hydrography programme limits the ability to constrain the year to year variability of the ocean carbon sink via the changes in the carbon storage.

Ocean carbon sink variability

Analyses of the sea-to-air fluxes of CO_2 are better suited to address the variability of the ocean carbon sink, as they can be used to analyse changes at much higher temporal resolutions. In addition, they also assess the potential contribution of the non-steady-state component of the natural CO_2 fluxes, which we expect to drive most of the ocean flux variability. The ability to constrain these sea-to-air CO_2 fluxes with observations has made large strides in the past decade for at least three reasons. The first was the expansion of the surface ocean partial pressure of CO_2 (pCO_2) measurement programmes that began in the 1960s (ref. 93) but picked up momentum in the late 1980s and 1990s (refs. 94–96). The second was the collation of the available surface ocean pCO_2 measurements by the Surface Ocean CO_2 Atlas (SOCAT) effort into a quality controlled and openly accessible data product[97–99]. More than 30 million observations are in the SOCAT V2022 release, but these observations cover only a small fraction of the ocean surface. For example, at any given month in the decade of the 2010s, only 3% of all 1° × 1° grid points of the surface ocean have at least one observation. Therefore, the last notable advance was the development of approaches to interpolate and extrapolate these surface ocean pCO_2 observations to obtain space–time continuous estimates of the sea-to-air CO_2 fluxes[100–102]. Six of these reconstructions have been harmonized into a globally consistent product[103], called SeaFlux.

The long-term mean fluxes of this ensemble are characterized by strong outgassing of CO_2 in equatorial regions, most prominently in the equatorial Pacific (Fig. 2). There is a strong net uptake of CO_2 at latitudes around 45° in both hemispheres. The overall pattern of the sources and sinks of CO_2 is primarily determined by the exchange of natural CO_2, responding to heating and cooling, vertical transport and mixing, and variations in biological productivity[9]. The uptake of anthropogenic CO_2 modifies these fluxes, most strongly in the areas of large uptake of anthropogenic CO_2 such as the tropics and the high latitudes[104].

There is an almost doubling of the global net sea-to-air flux of CO_2 estimated by the SeaFlux ensemble from around −1.5 Pg C $year^{-1}$ in 1990 to around −2.7 Pg C $year^{-1}$ in 2018 (Fig. 3a). A loss of natural CO_2 of 0.65 ± 0.30 Pg C $year^{-1}$ (ref. 105) needs to be subtracted from the ocean pCO_2-based estimates to compare these net fluxes with the global ocean uptake estimates here (Table 1) and also those reported by the Global Carbon Project[1,51]. This loss is part of a natural steady state of the global carbon cycle, and results from the difference between the carbon input by rivers and the carbon burial in marine sediments[105–108] (see also Box 1). After accounting for the outgassing of this river-derived carbon, the combined fluxes of steady-state anthropogenic CO_2 and non-steady-state natural and anthropogenic CO_2 are −2.1 ± 0.3 Pg C $year^{-1}$ in the 1990s, −2.3 ± 0.2 Pg C $year^{-1}$ in the 2000s and −3.1 ± 0.2 Pg C $year^{-1}$ in the 2010s (Table 1) (this flux is referred to as the ocean sink S_{OCEAN} in the Global Carbon Budget (GCB)[1,51]).

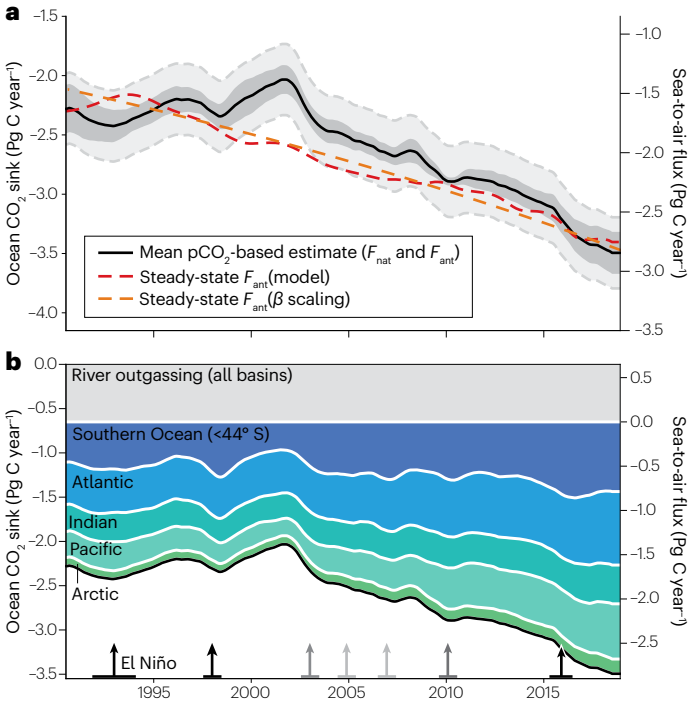

Fig. 3 | Temporal evolution of the global ocean CO_2 sink. a, Global ocean CO_2 sink estimated by the six ocean partial pressure of CO_2 (pCO_2) observation-based products contained in SeaFlux[103]. The estimated net sea-to-air fluxes were adjusted by the steady-state river outgassing flux of 0.65 Pg C $year^{-1}$ (ref. 105) to obtain the ocean CO_2 sink flux that is of relevance for balancing the global sources and sinks of CO_2 (the natural flux, F_{nat}, plus the anthropogenic flux, F_{ant}). Solid black line indicates the mean estimate, with the dark grey area representing the standard error across the six products. Dashed grey lines indicate the uncertainty of the ocean sink and include the uncertainty of ±0.30 Pg C $year^{-1}$ associated with the river outgassing flux[105]. Dashed red line represents the steady-state uptake of anthropogenic CO_2 estimated from a global ocean model (CESM-ETHZ[25]). Dashed orange line represents the expected steady-state uptake of anthropogenic CO_2 estimated from the sensitivity β (left axis). **b**, Contribution of the Southern Ocean and of individual ocean basins (north of 44° S) to the global ocean CO_2 sink based on the ensemble mean of the SeaFlux products. Grey band represents the steady-state oceanic outgassing of river-derived CO_2. It was not allocated to individual basins. El Niño events in the Pacific basin are represented by arrows, with grey shading indicating strength (darker arrows for stronger events). The global ocean carbon sink varies substantially in time around the long-term trend given by the steady-state uptake of anthropogenic CO_2 with a period of stagnant uptake in the 1990s followed by a period of faster than expected growth of the ocean carbon sink after the turn of the millennium.

Interannual to decadal variability

The overall trend from the 1990s to the present of about −0.4 Pg C $year^{-1}$ per decade is close to that estimated from the steady-state β-scaling for anthropogenic CO_2 (Fig. 3a, orange dashed line). The simulated fluxes from an ocean biogeochemical model run with constant circulation and constant biology (CESM-ETHZ)[25] show the same overall trend (Fig. 3a, red dashed line), although with some more variations, largely reflecting changes in the growth rate of atmospheric CO_2 (ref. 33). Thus, when analysed over the past three decades, the surface ocean fluxes suggest an ocean carbon sink that has increased at a rate commensurate with the steady-state prediction.

However, on interannual to decadal timescales, the ocean carbon sink diagnosed from the surface ocean pCO_2 observations deviates substantially from the steady-state prediction (Fig. 3a). The strongest deviations occur on decadal timescales, with a weakening sink during the 1990s (a decadal trend of +0.3 Pg C $year^{-1}$ per decade (1990–2001)), followed by a strong reinvigoration with a decadal trend of −0.7 Pg C $year^{-1}$ per decade (2002–2018), nearly twice the rate from the steady-state model. Integrated over the three decades, the ensemble mean uptake is 6 ± 5 Pg C (11%) smaller than expected from the steady-state prediction, that is, this difference suggests a non-steady-state or climate variability-induced loss of natural and anthropogenic CO_2. The estimates from the individual pCO_2-based reconstructions (Fig. 3a, grey region) vary substantially around the SeaFlux ensemble mean, but all agree on the strong decadal modulation of the ocean carbon sink around the long-term trend.

All ocean basins contribute to the decadal variations of the ocean carbon sink, but the largest changes occur in the Pacific Ocean and the Southern Ocean, which is defined here as the ocean south of 44° S[24,32,109,110] (Fig. 3b). Both basins experienced a strong minimum in uptake around 2002 and a recovery thereafter, whereas the Atlantic basin north of 44° S had a more gradual increase through time. The Pacific is the only basin that exhibits a clear interannual variability signal on top of the trend and the decadal changes. By contrast, the carbon sink of the Indian Ocean north of 44° S remained relatively constant.

Given that all these estimates rely on the same sparsely sampled pCO_2 data, however, the potential for systematic errors that transcends all interpolation methods cannot be excluded[111]. The reconstructions in the southern hemisphere are particularly concerning, as model-based analyses[111] suggest that the severe undersampling could lead to an overestimating of the diagnosed decadal variability. In addition, the cool surface ocean skin effect[112] and uncertainties associated with the functional dependence of the gas transfer velocity on wind and other environmental factors[113] add to the overall uncertainty of the flux products. Regardless, these variations — especially the weakening and strengthening periods — are seen in other, independent estimates, including from forward models[25] and inverse models[114], although with generally smaller magnitudes[23].

Patterns of variability

More details about the spatio-temporal nature of the sea-to-air flux variations can be gleaned from the results of ocean pCO_2 observation-based studies that emerged in the 2010s. A Hovmoeller plot of the zonal integrals of the anomalous air–sea fluxes (Fig. 4a) shows that the largest variations occur in the regions of strong absolute fluxes, that is, either in regions of strong uptake (temperate to high latitudes) or in the regions of strong outgassing of CO_2 (tropics). On top of the year to year variations, which are most prominent in the tropical latitudes, the long-term changes and the superimposed decadal variability clearly emerge from the data. They indicate that the extra-tropics (between 30° and 60° latitude) were the most important latitudes contributing to the rapid growth in the ocean carbon sink in the 2000s and 2010s, with the southern hemisphere dominating owing to its larger ocean surface area.

These fluxes are the sum of the anomalies of the anthropogenic and natural CO_2 flux components. To estimate the anomalies of the anthropogenic CO_2 flux, the steady-state estimates of the Ocean Inversion Project for the uptake of anthropogenic CO_2 (ref. 72) for the year 1995 were scaled to the entire period using the β-based scaling approach used above. The zonal integral of the anomalies of this CO_2 flux indicates that the regions of highest uptake in the Southern Ocean,

the tropics and the mid latitudes of the northern hemisphere imprint large trends on the fluxes in these regions. By contrast, other regions have only a small trend in absolute terms (Fig. 4b).

By removing this anthropogenic steady-state trend from the anomalous flux, the remaining anomalies reveal a clearer picture of the non-steady-state components driven by climate variability (Fig. 4c).

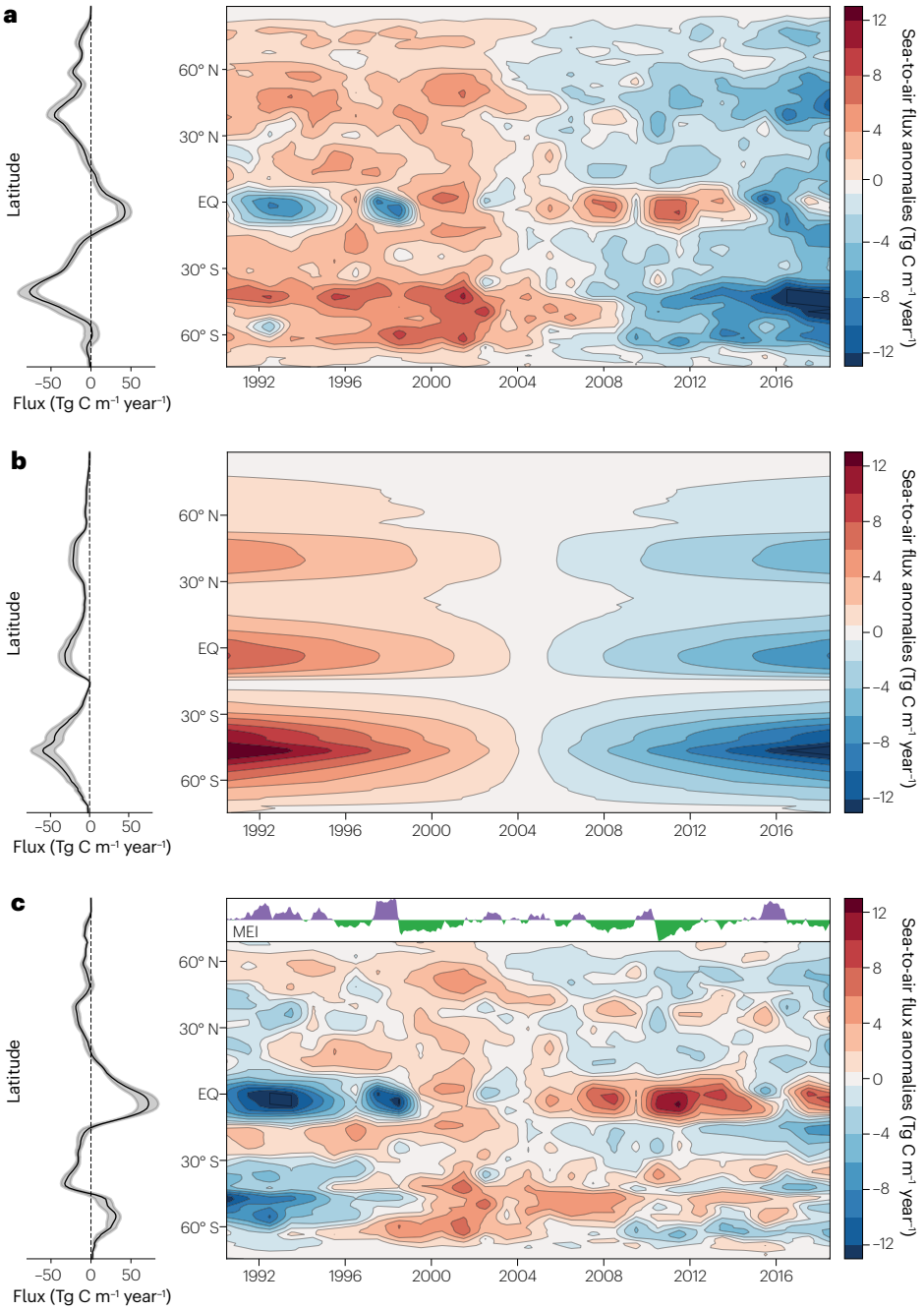

Fig. 4 | Zonally integrated anomalous CO_2 fluxes and their components. **a**, Hovmoeller diagram of the annual mean of the zonal mean anomalies of the total air–sea CO_2 fluxes as a function of time and latitude (right panels) together with the long-term (1990–2018) zonal mean fluxes (left panels). The anomalies were computed by subtracting the long-term mean flux from the annual mean flux for a given year using the ensemble mean data from the SeaFlux product[103]. The zonal mean dominates compared with the interannual variability. **b**, The same as panel **a** but for the long-term zonal mean (left panel) and anomalous air–sea fluxes of the steady-state component of anthropogenic CO_2. This estimate was obtained by scaling the ocean inversion-based estimate[72] for 1995 with a sensitivity β of 1.4 Pg C per ppm CO_2. The anomalies were then obtained by subtracting the long-term mean flux. **c**, The same as panel **a** but for the long-term zonal mean and anomalous air–sea fluxes of the non-steady-state component of CO_2, obtained by subtracting results in panel **b** from those in panel **a**. There is strong interannual variability of the air–sea fluxes in the tropics, largely associated with El Niño Southern Oscillation (ENSO) dynamics as indicated by the time series of the multivariate ENSO index (MEI)[115] in panel **c**, and the strong decadal variations in the Southern Ocean, largely driven by the non-steady-state components. EQ, equator.

The strong interannual nature of the variations in the tropical belt emerges even more prominently. These anomalies are correlated to the El Niño Southern Oscillation (ENSO), as indicated by the negative correlation of the zonal anomalies in the tropical belt with the multivariate ENSO index[115] ($R = -0.79$, $p < 0.05$). However, the anomalous uptake during El Niños was strong in the 1990s and weakened substantially after the turn of the millennium. At the same time, the anomalous outgassing during La Niña conditions strengthened over time. These ENSO-related trends yield a distinct decadal signal in the tropics as well, characterized by an anomalous uptake during the 1990s, neutral conditions during the first decade of the new millennium and anomalous outgassing in the 2010s.

The decadal nature of the Southern Ocean sink variability is also more discernible in these non-steady-state fluxes (Fig. 4c). Over the course of the 1990s, there was a rapid change from an anomalous uptake to an anomalous outgassing peaking around 2002. This was followed by a prolonged period of anomalous outgassing until about 2008 and a recovery to normal conditions around 2010. Thus, the strong trend in the Southern Ocean towards increasing uptake in the past two decades is largely the result of the strong trend imparted by the steady-state uptake of anthropogenic CO_2, reflecting the major role of this region in taking up anthropogenic CO_2 from the atmosphere[72,116] (Fig. 4b).

The trend from an anomalous sink to an anomalous source during the 1990s followed by a strengthening period after 2000 is also evident across most latitudes of the northern hemisphere (Fig. 4c). This co-occurrence suggests that apart from the tropics, the decadal mode of sea-to-air CO_2 flux variability has a global component, even after accounting for the steady-state trend in the uptake flux of anthropogenic CO_2.

In summary, the ocean pCO_2 observation-based constraints on the sea-to-air CO_2 fluxes that have emerged in the past decade have reshaped our understanding of the variability of the ocean carbon sink (Fig. 5). In particular, the surface flux products have suggested the presence of an important decadal mode of variability in the extra-tropics, and particularly in the Southern Ocean (Fig. 5). This observation contrasts with the results of ocean biogeochemical models, whose

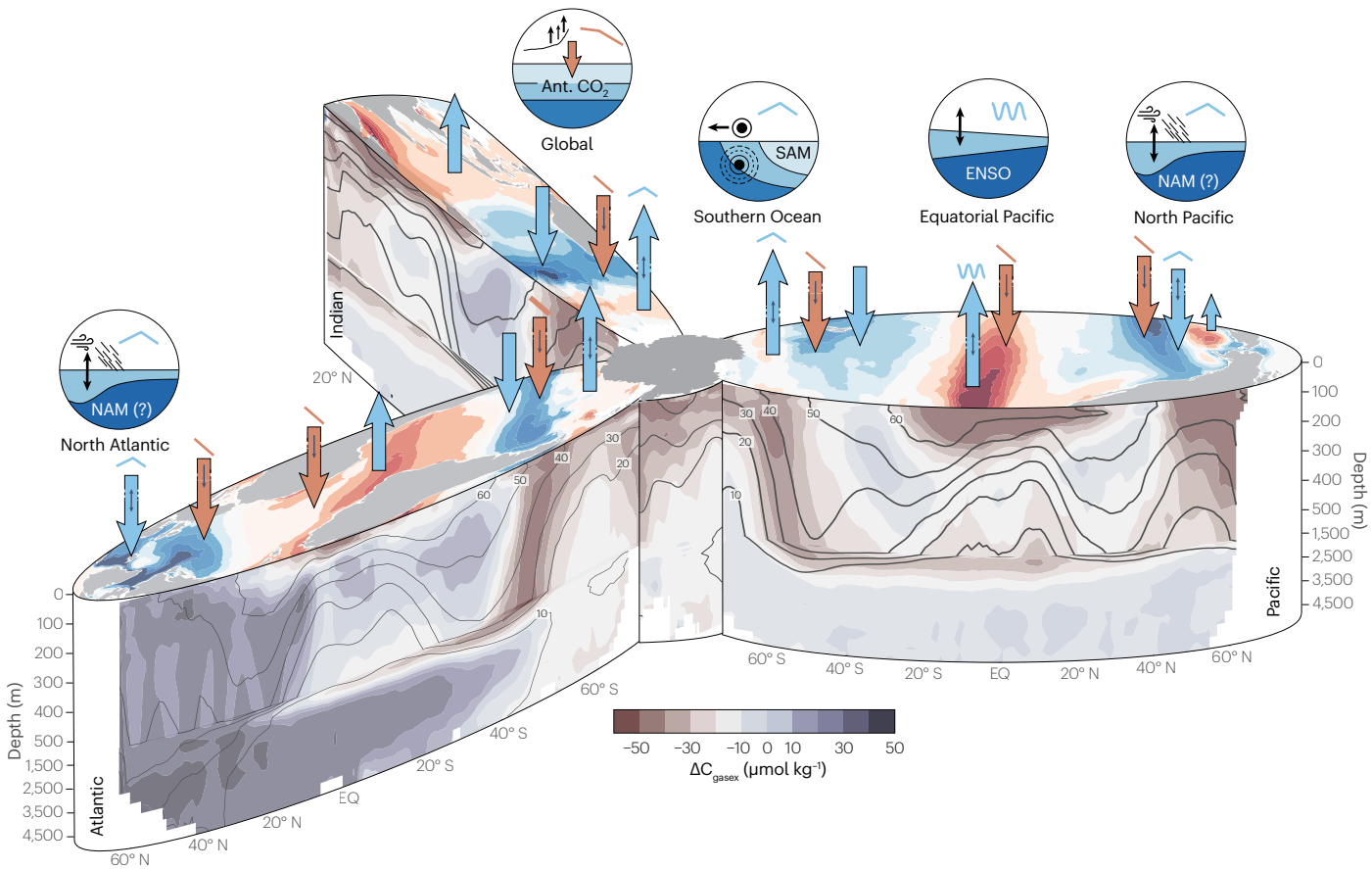

Fig. 5 | Interannual to decadal variability in the ocean carbon sink. The global ocean sources and sinks of CO_2 along the surface ocean. The ocean interior distribution of the gas exchange component of natural CO_2 (refs. 104,156) (colours) and of the total amount of anthropogenic CO_2 for 2007 (refs. 2,4) (isolines) are shown along the depth profile. The hot spots for interannual and decadal variability are noted by the icons. Gradients in the gas exchange component of natural CO_2 reflect the addition or removal of natural CO_2 through air–sea exchange at the surface. Turquoise arrows indicate the sea-to-air fluxes of natural CO_2 including the type and direction of variability (hat: decadal variability, waves: interannual variability). Reddish arrows indicate the oceanic uptake of anthropogenic CO_2, which is increasing everywhere (straight line). Not shown as arrows is the outgassing flux of the river-derived natural CO_2. The icons relate the variations in the dominant regions of variability (tropical Pacific, and the higher latitudes) to the underlying processes, such as El Niño Southern Oscillation (ENSO) in the tropical Pacific, and the high latitude modes of variability, especially the Southern Annular Mode (SAM) and the Northern Annular Mode (NAM). Changes in atmospheric CO_2 growth rates affect the global uptake of anthropogenic CO_2. EQ, equator; ΔC_{gasex}, change in C gas exchange.

variability tend to be, on average, smaller and also tend to have most of the variability focused in the tropics[25,30,117]. Nevertheless, the models also simulate decadal variability in the extra-tropics[23,25,28,29,118], adding further evidence that the decadal variability diagnosed from the observations is a robust feature.

Mechanisms of variability

Variations in the ocean carbon sink either can be caused by processes that are internal to the climate system or can be externally forced. Internal forcing is associated with variations in weather and climate[24,27,28,32,109,114,119], including changes associated with anthropogenic climate change[120]. External forcing is caused by changes outside the climate system, such as those induced by the volcanic eruption of Mount Pinatubo in 1991 (ref. 33). Such an eruption can impact the ocean carbon sink through changes in both Earth surface temperature and atmospheric CO_2 growth rate.

Interannual variations in the ocean carbon sink are driven by internal processes, as they are associated with the ENSO-related year to year variations in the sea-to-air fluxes in the tropical Pacific[30,121–123]. During El Niño conditions, reduced upwelling and thermocline deepening in the Eastern Tropical Pacific strongly decrease the vertical supply of DIC to the surface. This process causes a collapse of the high pCO_2 levels that drive CO_2 out of the ocean, even though sea-surface temperatures are warmer than normal. Reduced windspeeds during El Niño conditions tend to further reduce the outgassing and, thus, enhance the effect of the reduced supersaturation[123]. The resulting sea-to-air flux anomalies are sizable and impact the regional atmospheric CO_2 concentration[124]. The flux variations are most likely almost entirely driven by changes in the natural CO_2, in particular its non-steady-state component (Fig. 4c).

Mechanisms driving the decadal variations in the ocean carbon sink are less understood. One argument is that at least part of the variations are externally forced[33], as the eruption of Mount Pinatubo in 1991 caused both a reduced growth rate of atmospheric CO_2 during much of the 1990s (refs. 125–127) and a global cooling trend in the surface temperature. The low growth rate reduces the ocean carbon sink directly by modifying the air–sea pCO_2 gradient. This effect would be enhanced by the upper ocean cooling and the enhanced ocean mixing induced by this cooling[128,129]. According to this argument, these two processes would have reduced the oceanic uptake during the 1990s, whereas the resumption of higher atmospheric CO_2 growth rates thereafter would have caused the ocean uptake to rebound[33].

An alternative line of argument is that these decadal changes are the result of processes that are internal to the climate system. For example, a poleward contraction and intensification of the westerly wind belt around Antarctica might have caused the weakening trend of the Southern Ocean carbon sink during the 1990s (ref. 28), driven primarily by a trend towards a positive phase of the Southern Annular Mode (SAM)[130]. The stronger winds led to more upwelling of CO_2 and nutrient-rich deep water, increasing CO_2 outgassing (albeit partly balanced by stronger biological production)[28,118,131,132]. Then, a shift to a zonally more undulating wind field coupled with changes in sea-surface temperature caused the reinvigoration of the Southern Ocean carbon sink thereafter[32]. At least part of these wind changes, and especially those of the 1990s, have been attributed to anthropogenic warming and ozone loss forcing the positive trend in the SAM[133]. Simulations with ocean biogeochemical models suggest that the majority of the response of the CO_2 fluxes is driven by changes in the C_{nat}, with the fluxes of anthropogenic CO_2 modulating the response, often in opposite directions, thus moderating the effect[24,28,114,132].

In contrast to the Southern Ocean, the potential mechanisms causing the reconstructed increases in the carbon sink in the northern hemisphere after 2000 are not well investigated. The most likely mechanisms involve changes in winds, changes in temperature affecting the solubility, changes in buoyancy forcing affecting winter mixed layers[134] and large-scale gyre changes[27]. The latter are potentially associated with changes in the Northern Annular Mode (NAM) or associated northern hemisphere modes of variability[109].

The relative roles of internal versus external forcing driving the reconstructed decadal variations still need to be firmly established.

Glossary

Air–sea gas exchange
A diffusion-driven process governing the transfer of gases across the air–sea interface, driven by the concentration gradient of the gas across the interface and controlled by the level of turbulence at the interface.

Buffer factor
How well seawater is able to buffer an increase in surface ocean CO_2 (ocean partial pressure of CO_2), which is crucial for determining the amount of anthropogenic CO_2 the surface ocean can hold; also called the Revelle factor.

Dissolved inorganic carbon
(DIC). The sum of all dissolved inorganic carbon species in the seawater, including dissolved CO_2 (CO_2^{aq}), carbonic acid (H_2CO_3), bicarbonate (HCO_3^-) and carbonate (CO_3^{2-}).

El Niño Southern Oscillation
(ENSO). A quasi-periodic oscillation of the coupled ocean–atmosphere system with the majority of the action being focused on the eastern tropical Pacific; it is globally the dominant mode of climate variability.

External forcing
Processes leading to changes in the ocean carbon sink driven by processes external to the climate system, such as volcanic eruptions.

Forward models
A class of models that start from initial conditions and solve the governing balance equations by time-integrating them forward using a set of provided boundary conditions.

Inverse models
A class of models that fuse observations and models in order to improve our quantitative understanding of a set of processes.

Internal forcing
Processes leading to changes in the ocean carbon sink, primarily associated with (internally generated) weather and climate variations.

Ocean partial pressure of CO_2
(Ocean pCO_2). The partial pressure of CO_2 measured in the air in equilibrium with the water parcel under consideration at 1 atm total pressure and at the in situ temperature of the water parcel; often also referred to as pCO_2^{oc}.

Ocean acidification
Change in the ocean's seawater chemistry (pH, $[CO_3^{2-}]$, $CaCO_3$ saturation state and so on) as a consequence of the oceanic uptake of anthropogenic CO_2.

Ocean biogeochemical models
A class of ocean models where the most important biogeochemical processes are explicitly represented, namely air–sea gas exchange, chemical speciation and biological processes.

Southern Annular Mode
(SAM). A mode of variations in the polar atmosphere of the southern hemisphere, characterized by fluctuations in the strength of the circumpolar vortex.

Model simulations with a changing atmospheric CO_2 growth rate, but no changes in climate, suggest that the effect is visible, albeit much smaller than the observed changes (Fig. 3a, red versus orange dashed lines). The effect of the cooling and warming pattern associated with Mount Pinatubo is more difficult to quantify independently, but simulations with comprehensive ocean biogeochemical models[128,135] suggest an effect of ≤0.2 Pg C $year^{-1}$ during peak cooling, and rapidly decreasing thereafter. However, the ocean carbon sinks changing globally relatively synchronously supports that there was an external forcing mechanism (Fig. 4). Overall, external forcing (such as by volcanos) and internal changes (such as by weather and climate variability) are not mutually exclusive processes, and both likely play a role in driving ocean carbon sink variability.

Merging observational constraints

Bringing together the ocean interior constraints on the evolution of the ocean sink with those provided by the surface ocean measurements can help better understand the mechanisms driving trends and variability (Table 1). The estimates of the ocean interior accumulation of anthropogenic CO_2 suggest an ocean that globally has operated near steady state. The extrapolation with β-scaling suggests a cumulative uptake of about 83 Pg C between 1990 and 2019. The reconstructions of the surface fluxes, which include both natural and anthropogenic CO_2 components, suggest 6 ± 5 Pg C less uptake over the same period (Table 1 and Fig. 3a). This reduction is mostly attributed to a non-steady-state loss of natural CO_2, as the simulation with the observed variations in atmospheric CO_2 suggested a small change in the total uptake of anthropogenic CO_2 (Fig. 3, red dashed line). This loss needs to be taken into consideration when constructing global carbon budgets with ocean interior inventory changes. Indeed, a potential loss of 5 ± 3 Pg C was considered in the global assessment of the accumulation of anthropogenic CO_2 for the period 1994 through 2007 (ref. 4). In addition to circulation-driven decadal variability, part of this loss could be caused by ocean warming, as a warming-induced loss of 5 ± 1 Pg C between 1990 and 2020 (ref. 136) has been suggested (Table 1). These losses and the corresponding budget adjustments are currently very tentative, and urgently require verifications through direct observations of changes in the oceanic DIC pool, for example.

Although ocean interior and surface ocean constraints are becoming more consistent, new discrepancies have arisen. Most prominent is a growing difference between the ocean sink estimates based on surface ocean pCO_2 observations and those based on ocean biogeochemical models. These estimates agree well during the first decade of the millennium, but diverge thereafter, with the observation-based estimates indicating a much larger growth in the uptake than the models[1,25] (Table 1). This difference is also evident in these models yielding a relatively low sensitivity β of 1.11 ± 0.18 Pg C per ppm CO_2 for the period 1990 through 2019 (Fig. 1a; see Supplementary Table 1). One reason is that the presently used models tend to underestimate the uptake of anthropogenic CO_2, as evidenced by direct comparison with the uptake estimates stemming from the accumulation of anthropogenic CO_2 (ref. 1) (Fig. 1). A model-based emergent constraint approach on a different but related set of models suggests an underestimation of about 10%[137]. Adjusting the models for this bias halves the mismatch between models and observation-based estimates for the period after 2010, but opens larger discrepancies in the earlier decades. The uncertainties in the observation-based flux products stemming from the sparse observations, and issues at the tails of the observational-based time series[112], might contribute to these discrepancies.

Summary and future perspectives

The strength of the ocean carbon sink has tripled from the 1960s until the present. Thus, the ocean has maintained its key role as a sink for the CO_2 emitted into the atmosphere as a consequence of human activities, removing about 25 ± 2% of the total emissions over six decades. The strengthening of the ocean sink has been largely driven by the increasing uptake of anthropogenic CO_2 in response to the rise in atmospheric CO_2, leading to a strong proportionality between the two. By contrast, the contribution from changes in the natural carbon cycle has been small so far, consistent with the assumption that the ocean circulation and biological pump was overall in steady state. However, new insights and observations published in the past decade challenge this assumption, especially on shorter timescales, suggesting an ocean that is more variable than previously recognized. New evidence also suggests over the past three decades a loss of natural CO_2 to the atmosphere due to ocean warming and changes in ocean circulation. If confirmed, such a loss suggests an ocean carbon sink that is rather sensitive to climate change.

An ocean sink that is more sensitive to climate change than currently assumed in coupled carbon-climate models[52] would imply that the ocean will take up less CO_2 from the atmosphere in the future than anticipated. This would leave a larger fraction of the emissions in the atmosphere, causing additional global warming and climate change. In other words, the ocean carbon-climate feedback could be more positive than suggested by current coupled carbon-climate models. Moreover, the finding of the ocean sink potentially being more sensitive to changes in atmospheric CO_2 growth rates than previously recognized implies a stronger than anticipated decline of the ocean carbon sink in ambitious mitigation scenarios[34,138].

The implications are large and far-reaching. Any reduction in ocean carbon uptake compared with current assumptions would require even stronger investments into decarbonization strategies, making the achievement of specific global warming targets harder. It also reduces the efficacy of the negative emission approaches that aim to curb climate change by removing CO_2 from the atmosphere using land-based[139,140] or ocean-based[141] approaches.

To better constrain and predict the ocean carbon sink, there are three important challenges to address: the robustness of the reconstructed changes and variations; the processes driving these changes and variations; and predictions of the future ocean uptake, in particular the response of the ocean carbon sink to future climate change, the reduction in anthropogenic CO_2 emissions and the potential deployment of CO_2 removal technologies. Addressing these challenges is important both scientifically and for policy. For example, during the upcoming Global Stocktake undertaken within the UN Framework Convention on Climate Change (UNFCCC), reliable estimates of the ocean carbon sink will be a crucial element to close the global carbon budget. In addition, the study of ocean-based CO_2 removal approaches, such as ocean alkalinization, nutrient fertilization, seaweed growth and artificial upwelling, have gained momentum[141], requiring a thorough assessment of their effectiveness and consequences.

In our view, the following measures must be taken to answer these challenges (see also ref. 142). The existing observation networks need to be improved, expanded and put on a much better long-term funding level. The limited sampling of the ocean carbon system is currently the largest source of uncertainty in assessing the variability of the ocean carbon sink. The current sampling is sufficient to capture the long-term time mean sink, and the year to year variations in the tropical Pacific and a few other regions, especially in the northern hemisphere where the

sampling is relatively dense. By contrast, sampling is critical in many other key regions, such as the Southern Ocean, the South Pacific and the Indian Ocean. Higher resolution observations in time and space will also help better understand the processes leading to these variations, including those that lead to extremes in ocean acidification and/or deoxygenation[143]. Ocean-observing system simulation experiments can help determine where and when the observing density has to be increased, and to suggest optimal combinations of different observing platforms[144,145].

To support observation, new technologies — especially those that enhance the ability to observe ocean carbon in an autonomous manner — need to be developed, improved and strategically deployed. Improvement of analytical techniques, sensor technology and calibration methods for ocean carbon measurements is urgently required for the provision of accurate, well-calibrated ocean carbon measurements. At the same time, the ease and efficiency of data collection needs to be improved, thus increasing the scope for autonomous data collection and reducing the cost of these measurements, such as the Biogeochemical Argo programme[146–148].

To build on expanded and improved sampling, the existing ocean carbon synthesis projects (GLODAP and SOCAT) and the downstream efforts such as the GCB and SeaFlux need to be strengthened and expanded. A more rapid update of the analyses, such as on a semi-annual basis providing closer to real-time analyses of the global carbon budget, could be useful to better link the ocean to the Global Stocktake activities. Similarly, models and observations need to be better integrated, especially through data assimilation and interpolation approaches[149–151]. As part of this effort, these inverse models should be pushed to resolve smaller spatial and temporal scales, better capturing the small-scale variability that is inherent in the data that are collected and assimilated by these models. If these models can resolve both the large scales that are representative of global budgets and the small scales that are representative of the observations, they will be able to more accurately reflect our state of knowledge and its uncertainty.

Moving beyond carbon measurements and budgets, focused process studies need to be developed to better understand critical processes. The need to improve knowledge of the sensitivity of ocean biology to changes in temperature, ocean acidification and other parameters is pressing. In addition, researchers need a better understanding of the aquatic continuum[105] — the aquatic network that connects the land aquatic systems to the ocean, delivering inorganic and organic matter to the ocean, whose fate is critical to determine the outgassing of river-derived CO_2. Although a value of 0.65 Pg C year^{-1} for the degassing of terrestrially derived CO_2 was used here and in the GCB[1], individual estimates range between 0.2 Pg C year^{-1} (ref. 152) and 1.2 Pg C year^{-1} (ref. 153), reflecting the large uncertainty of this estimate. An especially under-investigated area is the fate of the river-derived carbon in the ocean, and in particular the determination of how much carbon is buried in sediments close to the river mouths, how much enters the open ocean and how fast this carbon is remineralized back to CO_2 (ref. 152).

The role of the ocean in taking up additional CO_2 in response to the deployment of CO_2 removal technologies needs to be critically evaluated. There must be a particular focus on the efficacy of these measures and their potential for negative (unintended) consequences[154]. Historically, the ocean sink for carbon has been considered as very robust to changes, and largely tracking the increase in atmospheric CO_2. It is time to change this perspective and to recognize that the ocean carbon cycle might be more sensitive to change than previously recognized. The size of this sink, its unknown response to a reduction in anthropogenic CO_2 emissions and its relevance for past and future climates are large enough to warrant renewed efforts to observe it, to study it and to understand it.

Published online: 24 January 2023

References

1. Friedlingstein, P. et al. Global Carbon Budget 2021. *Earth Syst. Sci. Data* **14**, 1917–2005 (2022).
This work is the most recent version of the GCB, an international effort led by the Global Carbon Project to synthesize all components of the global carbon cycle.
2. Sabine, C. L. et al. The oceanic sink for anthropogenic CO_2. *Science* **305**, 367–371 (2004).
This work is the first observation-based global inventory of anthropogenic CO_2 providing a key constraint for the global anthropogenic CO_2 budget.
3. Khatiwala, S., Primeau, F. & Hall, T. Reconstruction of the history of anthropogenic CO_2 concentrations in the ocean. *Nature* **462**, 346–349 (2009).
This work reconstructs the entire history of the oceanic uptake of anthropogenic CO_2.
4. Gruber, N. et al. The oceanic sink for anthropogenic CO_2 from 1994 to 2007. *Science* **363**, 1193–1199 (2019).
This work presents an inventory of anthropogenic CO_2 that provided a second time point describing the accumulation of anthropogenic CO_2 in the ocean based on ocean interior observations.
5. Revelle, R. in *The Global Carbon Cycle and Atmospheric CO_2: Natural Variations Archean to Present* (eds Sundquist, E. T. & Broecker, W. S.) 1–4 (AGU, 1985).
6. Heimann, M. A review of the contemporary global carbon cycle and as seen a century ago by Arrhenius and Hogbom. *Ambio* **26**, 17–24 (1997).
7. Arrhenius, S. *Lehrbuch der kosmischen Physik* Vol. 2 (Hirzel, 1903).
8. Archer, D., Kheshgi, H. & Maier-Reimer, E. Multiple timescales for neutralization of fossil fuel CO_2. *Geophys. Res. Lett.* **24**, 405–408 (1997).
9. Sarmiento, J. L. & Gruber, N. *Ocean Biogeochemical Dynamics* (Princeton Univ. Press, 2006).
10. Callendar, G. S. The artificial production of carbon dioxide and its influence on climate. *Q. J. R. Meteor. Soc.* **64**, 223–240 (1938).
11. Revelle, R. & Suess, H. E. Carbon dioxide exchange between atmosphere and ocean and the question of an increase of atmospheric CO_2 during the past decades. *Tellus* **9**, 18–27 (1957).
12. Revelle, R., Broecker, W. S., Craig, H., Keeling, C. D. & Smagorinsky, J. in *Restoring the Quality of Our Environment. Appendix Y4: Atmospheric Carbon Dioxide* 111–133 (US Gov. Printing Office, 1965).
13. Charney, J. G. et al. *Carbon Dioxide and Climate: A Scientific Assessment* (National Academy of Sciences, 1979).
14. Keeling, C. D. The concentration and isotopic abundances of carbon dioxide in the atmosphere. *Tellus* **12**, 200–203 (1960).
15. Wallace, D. W. R. in *Ocean Circulation and Climate* Ch. 6.3 (eds Siedler, G., Church, J. & Gould, J.) 489–521, XLIX-L (Academic, 2001).
16. Keppler, L., Landschützer, P., Gruber, N., Lauvset, S. K. & Stemmler, I. Seasonal carbon dynamics in the near-global ocean. *Glob. Biogeochem. Cycles* **34**, e2020GB006571 (2020).
17. Canadell, P. G. et al. in *Climate Change 2021: The Physical Science Basis. Contribution of Working Group I to the Sixth Assessment Report of the Intergovernmental Panel on Climate Change* (eds Masson-Delmotte, V. et al.) 673–816 (IPCC, 2021).
18. Oeschger, H., Siegenthaler, U., Schotterer, U. & Gugelmann, A. A box diffusion model to study the carbon dioxide exchange in nature. *Tellus* **27**, 168–192 (1975).
19. Brewer, P. G. Direct observation of the oceanic CO_2 increase. *Geophys. Res. Lett.* **5**, 997–1000 (1978).
20. Chen, C.-T. A. & Millero, F. J. Gradual increase of oceanic CO_2. *Nature* **277**, 205–206 (1979).
21. Sabine, C. L. & Tanhua, T. Estimation of anthropogenic CO_2 inventories in the ocean. *Ann. Rev. Mar. Sci.* **2**, 175–198 (2010).
22. Olsen, A. et al. The Global Ocean Data Analysis Project version 2 (GLODAPv2)—an internally consistent data product for the world ocean. *Earth Syst. Sci. Data* **8**, 297–323 (2016).
23. DeVries, T. et al. Decadal trends in the ocean carbon sink. *Proc. Natl Acad. Sci. USA* **116**, 201900371 (2019).
24. Gruber, N., Landschützer, P. & Lovenduski, N. S. The variable Southern Ocean carbon sink. *Ann. Rev. Mar. Sci.* **11**, 159–186 (2019).
25. Hauck, J. et al. Consistency and challenges in the ocean carbon sink estimate for the global carbon budget. *Front. Mar. Sci.* **7**, 1–33 (2020).
This work describes and assesses the ocean biogeochemical models currently used to determine the oceanic uptake of CO_2 in the context of the GCB.
26. Landschützer, P., Gruber, N., Bakker, D. C. E. & Schuster, U. Recent variability of the global ocean carbon sink. *Glob. Biogeochem. Cycles* **28**, 927–949 (2014).
27. Landschützer, P., Gruber, N. & Bakker, D. C. E. Decadal variations and trends of the global ocean carbon sink. *Glob. Biogeochem. Cycles* **30**, 1396–1417 (2016).
28. Le Quere, C. et al. Saturation of the Southern Ocean CO_2 sink due to recent climate change. *Science* **316**, 1735–1738 (2007).

29. Lovenduski, N. S., Gruber, N., Doney, S. C. & Lima, I. D. Enhanced CO_2 outgassing in the Southern Ocean from a positive phase of the Southern Annular Mode. *Global Biogeochem. Cycles* https://doi.org/10.1029/2006GB002900 (2007).
30. Le Quéré, C., Orr, J. C., Monfray, P., Aumont, O. & Madec, G. Interannual variability of the oceanic sink of CO_2 from 1979 through 1997. *Glob. Biogeochem. Cycles* **14**, 1247–1265 (2000).
This study is the first to point out that the Southern Ocean carbon sink weakened substantially during the 1990s.
31. Fay, A. R. & McKinley, G. A. Global trends in surface ocean pCO_2 from in situ data. *Glob. Biogeochem. Cycles* **27**, 541–557 (2013).
32. Landschützer, P. et al. The reinvigoration of the Southern Ocean carbon sink. *Science* **349**, 1221–1224 (2015).
This work assesses the decadal variability of the ocean carbon sink and reveals it is driven by the extratropical latitudes in both hemispheres.
33. McKinley, G. A., Fay, A. R., Eddebbar, Y. A., Gloege, L. & Lovenduski, N. S. External forcing explains recent decadal variability of the ocean carbon sink. *AGU Adv.* **1**, 1–10 (2020).
34. Rogelj, J. et al. in *Global Warming of 1.5 °C. An IPCC Special Report* 93–174 (IPCC, 2018).
35. Cheng, L. et al. Another record: ocean warming continues through 2021 despite La Niña conditions. *Adv. Atmos. Sci.* https://doi.org/10.1007/s00376-022-1461-3 (2022).
36. Abram, N. et al. in *Special Report on the Ocean and Cryosphere (SROCC)* Ch. 1 (eds Pörtner, H.-O. et al.) (IPCC, 2019).
37. Bindoff, N. L. et al. in *Special Report on the Ocean and Cryosphere (SROCC)* Ch. 5 (eds Pörtner, H.-O. et al.) (IPCC, 2019).
38. Sarmiento, J. L., Orr, J. C. & Siegenthaler, U. A perturbation simulation of CO_2 uptake in an ocean general circulation model. *J. Geophys. Res.* **97**, 3621–3645 (1992).
39. Matsumoto, K. Radiocarbon-based circulation age of the world oceans. *J. Geophys. Res.* **112**, 1–7 (2007).
40. Holzer, M. & Primeau, F. W. The path-density distribution of oceanic surface-to-surface transport. *J. Geophys. Res. Ocean.* **113**, 1–22 (2008).
41. Dong, Y. et al. Update on the temperature corrections of global air–sea CO_2 flux estimates. *Glob. Biogeochem. Cycles* **26**, 21–35 (2022).
42. Matsumoto, K. & Gruber, N. How accurate is the estimation of anthropogenic carbon in the ocean? An evaluation of the ΔC* method. *Glob. Biogeochem. Cycles* https://doi.org/10.1029/2004GB002397 (2005).
43. Bates, N. et al. A time-series view of changing ocean chemistry due to ocean uptake of anthropogenic CO_2 and ocean acidification. *Oceanography* **27**, 126–141 (2014).
44. Gregor, L. & Gruber, N. OceanSODA-ETHZ: a global gridded data set of the surface ocean carbonate system for seasonal to decadal studies of ocean acidification. *Earth Syst. Sci. Data* **13**, 777–808 (2021).
45. Broecker, W. S., Takahashi, T., Simpson, H. J. & Peng, T. H. Fate of fossil fuel carbon dioxide and the global carbon budget. *Science* **206**, 409–418 (1979).
46. Egleston, E. S., Sabine, C. L. & Morel, F. M. M. Revelle revisited: buffer factors that quantify the response of ocean chemistry to changes in DIC and alkalinity. *Glob. Biogeochem. Cycles* **24**, 1–9 (2010).
47. Jiang, L. Q., Carter, B. R., Feely, R. A., Lauvset, S. K. & Olsen, A. Surface ocean pH and buffer capacity: past, present and future. *Sci. Rep.* **9**, 18624 (2019).
48. Sarmiento, J. L., LeQuéré, C. & Pacala, S. W. Limiting future atmospheric carbon dioxide. *Glob. Biogeochem. Cycles* **9**, 121–137 (1995).
49. Joos, F. et al. An efficient and accurate representation of complex oceanic and biospheric models of anthropogenic carbon uptake. *Tellus* **48B**, 397–417 (1996).
50. Keeling, C. D. The Suess effect: ^{13}-carbon and ^{14}-carbon interactions. *Environment Int.* **2**, 229–300 (1979).
51. Friedlingstein, P. et al. Global Carbon Budget 2020. *Earth Syst. Sci. Data* **12**, 3269–3340 (2020).
52. Arora, V. K. et al. Carbon–concentration and carbon–climate feedbacks in CMIP6 models and their comparison to CMIP5 models. *Biogeosciences* **17**, 4173–4222 (2020).
53. Friedlingstein, P. et al. Climate-carbon cycle feedback analysis: results from the C4MIP model intercomparison. *J. Clim.* **19**, 3337–3353 (2006).
54. Meinshausen, M. et al. Realization of Paris Agreement pledges may limit warming just below 2 °C. *Nature* **604**, 304–309 (2022).
55. Joos, F. et al. Carbon dioxide and climate impulse response functions for the computation of greenhouse gas metrics: a multi-model analysis. *Atmos. Chem. Phys.* **13**, 2793–2825 (2013).
56. Waugh, D. W., Hall, T. M., Mcneil, B. I., Key, R. & Matear, R. J. Anthropogenic CO_2 in the oceans estimated using transit time distributions. *Tellus B Chem. Phys. Meteorol.* **58**, 376–389 (2006).
57. Tanhua, T. et al. Ventilation of the Arctic Ocean: mean ages and inventories of anthropogenic CO_2 and CFC-11. *J. Geophys. Res.* **114**, 1–11 (2009).
58. Raimondi, L., Tanhua, T., Azetsu-Scott, K., Yashayaev, I. & Wallace, D. W. R. A 30-year time series of transient tracer-based estimates of anthropogenic carbon in the Central Labrador Sea. *J. Geophys. Res. Ocean.* **126**, 1–19 (2021).
59. Ridge, S. M. & McKinley, G. A. Ocean carbon uptake under aggressive emission mitigation. *Biogeosciences* **18**, 2711–2725 (2021).
60. Archer, D., Kheshgi, H. & Maier-Reimer, E. Dynamics of fossil fuel CO_2 neutralization by marine $CaCO_3$. *Glob. Biogeochem. Cycles* **12**, 259–276 (1998).
61. Bacastow, R. B. & Keeling, C. D. in *Workshop on the Global Effects of Carbon Dioxide from Fossil Fuels* (eds. Elliott, W. P. & Machta, L.) 72–90 (US Dept. of Energy, 1979).
62. Siegenthaler, U. & Oeschger, H. Predicting future atmospheric carbon dioxide levels. *Science* **199**, 388–395 (1978).
63. Wallace, D. W. R. *Monitoring Global Ocean Carbon Inventories* (Ocean Observing System Development Panel, 1995).
64. Gruber, N., Sarmiento, J. L. & Stocker, T. F. An improved method for detecting anthropogenic CO_2 in the oceans. *Glob. Biogeochem. Cycles* **10**, 809–837 (1996).
65. Gruber, N. Anthropogenic CO_2 in the Atlantic Ocean. *Glob. Biogeochem. Cycles* **12**, 165–191 (1998).
66. Dickson, A. G. & Goyet, C. Handbook of methods for the analysis of the various parameters of the carbon dioxide system in sea water; version 2. *OSTI* https://www.osti.gov/biblio/10107773 (1994).
67. Dickson, A. G., Afghan, J. D. & Anderson, G. C. Reference materials for oceanic CO_2 analysis: a method for the certification of total alkalinity. *Mar. Chem.* **80**, 185–197 (2003).
68. Dickson, A. G. Standards for ocean measurements. *Oceanography* **23**, 34–47 (2010).
69. Key, R. M. et al. A global ocean carbon climatology: results from Global Data Analysis Project (GLODAP). *Glob. Biogeochem. Cycles* https://doi.org/10.1029/2004GB002247 (2004).
70. DeVries, T. The oceanic anthropogenic CO_2 sink: storage, air–sea fluxes, and transports over the industrial era. *Glob. Biogeochem. Cycles* **28**, 631–647 (2014).
71. Orr, J. C. et al. Estimates of anthropogenic carbon uptake from four three-dimensional global ocean models. *Glob. Biogeochem. Cycles* **15**, 43–60 (2001).
72. Mikaloff Fletcher, S. E. et al. Inverse estimates of anthropogenic CO_2 uptake, transport, and storage by the ocean. *Glob. Biogeochem. Cycles* **20**, 1–16 (2006).
This ocean inversion-based study describes the regional distribution of the air–sea fluxes of anthropogenic CO_2 and its oceanic transport.
73. Davila, X. et al. How is the ocean anthropogenic carbon reservoir filled? *Glob. Biogeochem. Cycles* **36**, 1–16 (2022).
74. Groeskamp, S., Lenton, A., Matear, R., Sloyan, B. M. & Langlais, C. Anthropogenic carbon in the ocean—surface to interior connections. *Glob. Biogeochem. Cycles* **30**, 1682–1698 (2016).
75. Keeling, R. F. & Shertz, S. R. Seasonal and interannual variations in atmospheric oxygen and implications for the global carbon cycle. *Nature* **358**, 723–727 (1992).
76. Quay, P. D., Tilbrook, B. & Wong, C. S. Oceanic uptake of fossil fuel CO_2: carbon-13 evidence. *Science* **256**, 74–79 (1992).
77. Heimann, M. & Maier-Reimer, E. On the relations between the oceanic uptake of CO_2 and its carbon isotopes. *Glob. Biogeochem. Cycles* **10**, 89–110 (1996).
78. Gruber, N. & Keeling, C. D. An improved estimate of the isotopic air–sea disequilibrium of CO_2: implications for the oceanic uptake of anthropogenic CO_2. *Geophys. Res. Lett.* **28**, 555–558 (2001).
79. Khatiwala, S. et al. Global ocean storage of anthropogenic carbon. *Biogeosciences* **10**, 2169–2191 (2013).
80. Friedrich, T. et al. Detecting regional anthropogenic trends in ocean acidification against natural variability. *Nature* **2**, 167–171 (2012).
81. Munro, D. R. et al. Recent evidence for a strengthening CO_2 sink in the Southern Ocean from carbonate system measurements in the Drake Passage (2002–2015). *Geophys. Res. Lett.* **42**, 7623–7630 (2015).
82. Talley, L. D. et al. Changes in ocean heat, carbon content, and ventilation: a review of the first decade of GO-SHIP global repeat hydrography. *Ann. Rev. Mar. Sci.* **8**, 185–215 (2016).
83. Wanninkhof, R. et al. Detecting anthropogenic CO_2 changes in the interior Atlantic Ocean between 1989 and 2005. *J. Geophys. Res.* **115**, C11028 (2010).
84. Friis, K., Körtzinger, A., Pätsch, J. & Wallace, D. W. R. On the temporal increase of anthropogenic CO_2 in the subpolar North Atlantic. *Deep. Res. Part I* **52**, 681–698 (2005).
85. Goodkin, N. F., Levine, N. M., Doney, S. C. & Wanninkhof, R. Impacts of temporal CO_2 and climate trends on the detection of ocean anthropogenic CO_2 accumulation. *Glob. Biogeochem. Cycles* **25**, 1–11 (2011).
86. Levine, N. M., Doney, S. C., Wanninkhof, R., Lindsay, K. & Fung, I. Y. Impact of ocean carbon system variability on the detection of temporal increases in anthropogenic CO_2. *J. Geophys. Res.* **113**, C03019 (2008).
87. Carter, B. R. et al. Two decades of Pacific anthropogenic carbon storage and ocean acidification along Global Ocean Ship-based Hydrographic Investigations Program sections P16 and P02. *Glob. Biogeochem. Cycles* **31**, 306–327 (2017).
88. Carter, B. R. et al. Pacific anthropogenic carbon between 1991 and 2017. *Glob. Biogeochem. Cycles* https://doi.org/10.1029/2018GB006154 (2019).
89. Woosley, R. J., Millero, F. J. & Wanninkhof, R. Rapid anthropogenic changes in CO_2 and pH in the Atlantic Ocean: 2003–2014. *Glob. Biogeochem. Cycles* **30**, 70–90 (2016).
90. Clement, D. & Gruber, N. The eMLR(C*) method to determine decadal changes in the global ocean storage of anthropogenic CO_2. *Glob. Biogeochem. Cycles* **32**, 654–679 (2018).
91. Tanhua, T., Körtzinger, A., Friis, K., Waugh, D. W. & Wallace, D. W. R. An estimate of anthropogenic CO_2 inventory from decadal changes in oceanic carbon content. *Proc. Natl. Acad. Sci. USA* **104**, 3037–3042 (2007).
92. Pérez, F. F. et al. Atlantic Ocean CO_2 uptake reduced by weakening of the meridional overturning circulation. *Nat. Geosci.* **6**, 146–152 (2013).
93. Keeling, C. D. Carbon dioxide in surface ocean waters: 4. Global distribution. *J. Geophys. Res.* **73**, 4543–4553 (1968).
94. Tans, P. P., Fung, I. Y. & Takahashi, T. Observational contrains on the global atmospheric CO_2 budget. *Science* **247**, 1431–1438 (1990).
95. Takahashi, T. et al. Global air–sea flux of CO_2: an estimate based on measurements of sea–air pCO_2 difference. *Proc. Natl Acad. Sci. USA* **94**, 8292–8299 (1997).

96. Takahashi, T. et al. Deep-sea research II climatological mean and decadal change in surface ocean pCO_2, and net sea–air CO_2 flux over the global oceans. *Deep-Sea Res. II Top. Stud. Oceanogr.* **56**, 554–577 (2009).
97. Bakker, D. C. E. et al. An update to the Surface Ocean CO_2 Atlas (SOCAT version 2). *Earth Syst. Sci. Data* **6**, 69–90 (2014).
98. Pfeil, B. et al. A uniform, quality controlled Surface Ocean CO_2 Atlas (SOCAT). *Earth Syst. Sci. Data* **5**, 125–143 (2013).
99. Bakker, D. C. E. et al. A multi-decade record of high-quality CO_2 data in version 3 of the Surface Ocean CO_2 Atlas (SOCAT). *Earth Syst. Sci. Data* **8**, 383–413 (2016).
100. Rödenbeck, C. et al. Data-based estimates of the ocean carbon sink variability—first results of the Surface Ocean pCO_2 Mapping intercomparison (SOCOM). *Biogeosciences* **12**, 7251–7278 (2015).
101. Landschützer, P. et al. A neural network-based estimate of the seasonal to inter-annual variability of the Atlantic Ocean carbon sink. *Biogeosciences* **10**, 7793–7815 (2013).
102. Gregor, L., Lebehot, A. D., Kok, S. & Scheel Monteiro, P. M. A comparative assessment of the uncertainties of global surface ocean CO_2 estimates using a machine-learning ensemble (CSIR-ML6 version 2019a)—have we hit the wall? *Geosci. Model. Dev.* **12**, 5113–5136 (2019).
103. Fay, A. R. et al. SeaFlux: harmonization of air–sea CO_2 fluxes from surface pCO_2 data products using a standardized approach. *Earth Syst. Sci. Data* **13**, 4693–4710 (2021).
104. Gruber, N. et al. Oceanic sources, sinks, and transport of atmospheric CO_2. *Glob. Biogeochem. Cycles* **23**, https://doi.org/10.1029/2008GB003349 (2009).
105. Regnier, P., Resplandy, L., Najjar, R. G. & Ciais, P. The land-to-ocean loops of the global carbon cycle. *Nature* **603**, 401–410 (2022).
106. Sarmiento, J. L. & Sundquist, E. T. Revised budget for the oceanic uptake of anthropogenic carbon dioxide. *Nature* **356**, 589–593 (1992).
107. Regnier, P. et al. Anthropogenic perturbation of the carbon fluxes from land to ocean. *Nat. Geosci.* **6**, 597–607 (2013).
108. Resplandy, L. et al. Revision of global carbon fluxes based on a reassessment of oceanic and riverine carbon transport. *Nat. Geosci.* **11**, 504–509 (2018).
109. Landschützer, P., Ilyina, T. & Lovenduski, N. S. Detecting regional modes of variability in observation-based surface ocean pCO_2. *Geophys. Res. Lett.* **46**, 2670–2679 (2019).
110. Ritter, R. et al. Observation-based trends of the Southern Ocean carbon sink. *Geophys. Res. Lett.* **44**, 12,339–12,348 (2017).
111. Gloege, L. et al. Quantifying errors in observationally-based estimates of ocean carbon sink variability. *Glob. Biogeochem. Cycles* https://doi.org/10.1029/2020gb006788 (2021).
112. Watson, A. J. et al. Revised estimates of ocean–atmosphere CO_2 flux are consistent with ocean carbon inventory. *Nat. Commun.* **11**, 1–6 (2020).
113. Wanninkhof, R., Asher, W. E., Ho, D. T., Sweeney, C. & Mcgillis, W. R. Advances in quantifying air-sea gas exchange and environmental forcing. *Ann. Rev. Mar. Sci.* **1**, 213–244 (2009).
114. DeVries, T., Holzer, M. & Primeau, F. Recent increase in oceanic carbon uptake driven by weaker upper-ocean overturning. *Nature* **542**, 215–218 (2017).
115. Wolter, K. & Timlin, M. S. El Niño/Southern Oscillation behaviour since 1871 as diagnosed in an extended multivariate ENSO index (MEI.ext). *Int. J. Climatol.* **31**, 1074–1087 (2011).
116. Frölicher, T. L. et al. Dominance of the Southern Ocean in anthropogenic carbon and heat uptake in CMIP5 models. *J. Clim.* **28**, 862–886 (2015).
117. McKinley, G. A., Rödenbeck, C., Gloor, M., Houweling, S. & Heimann, M. Pacific dominance to global air–sea CO_2 flux variability: a novel atmospheric inversion agrees with ocean models. *Geophys. Res. Lett.* **31**, 10.1029/2004GL021069 (2004).
118. Lenton, A. & Matear, R. J. Role of the Southern Annular Mode (SAM) in Southern Ocean CO_2 uptake. *Glob. Biogeochem. Cycles* **21**, 1–17 (2007).
119. Keppler, L. & Landschützer, P. Regional wind variability modulates the Southern Ocean carbon sink. *Sci. Rep.* **9**, 7384 (2019).
120. Le Quéré, C., Takahashi, T., Buitenhuis, E. T., Rödenbeck, C. & Sutherland, S. C. Impact of climate change and variability on the global oceanic sink of CO_2. *Glob. Biogeochem. Cycles* **24**, https://doi.org/10.1029/2009GB003599 (2010).
121. Feely, R. A., Wanninkhof, R., Takahashi, T. & Tans, P. Influence of El Niño on the equatorial Pacific contribution to atmospheric CO_2 accumulation. *Nature* **398**, 597–601 (1999).
122. Ishii, M. et al. Air–sea CO_2 flux in the Pacific Ocean for the period 1990–2009. *Biogeosciences* **11**, 709–734 (2014).
123. McKinley, G. A., Follows, M. J. & Marshall, J. Mechanisms of air–sea CO_2 flux variability in the equatorial Pacific and the North Atlantic. *Glob. Biogeochem. Cycles* https://doi.org/10.1029/2003GB002179 (2004).
124. Chatterjee, A. et al. Influence of El Niño on atmospheric CO_2 over the tropical Pacific Ocean: findings from NASA's OCO-2 mission. *Science.* **358**, eaam5776 (2017).
125. Keeling, C. D., Whorf, T. P., Wahlen, M. & Plicht, J. V. D. Interannual extremes in the rate of atmospheric carbon dioxide since 1980. *Nature* **375**, 666–670 (1995).
126. Crisp, D. et al. How well do we understand the land–ocean–atmosphere carbon cycle. *Rev. Geophys.* https://doi.org/10.1029/2021rg000736 (2022).
127. Angert, A., Biraud, S., Bonfils, C., Buermann, W. & Fung, I. CO_2 seasonality indicates origins of post-Pinatubo sink. *Geophys. Res. Lett.* **31**, 1999–2002 (2004).
128. Eddebbar, Y. A. et al. El Niño-like physical and biogeochemical ocean response to tropical eruptions. *J. Clim.* **32**, 2627–2649 (2019).
129. Marshall, L. R. et al. Volcanic effects on climate: recent advances and future avenues. *Bull. Volcanol.* **84**, 54 (2022).
130. Thompson, D. W. J. & Solomon, S. Interpretation of recent southern hemisphere climate change. *Science* **296**, 895–899 (2002).
131. Hauck, J. et al. Seasonally different carbon flux changes in the Southern Ocean in response to the Southern Annular Mode. *Glob. Biogeochem. Cycles* **27**, 1236–1245 (2013).
132. Lovenduski, N. S., Gruber, N. & Doney, S. C. Toward a mechanistic understanding of the decadal trends in the Southern Ocean carbon sink. *Glob. Biogeochem. Cycles* **22**, 1–9 (2008).
133. Gillett, N. P. & Thompson, D. W. J. Simulation of recent southern hemisphere climate change. *Science* **302**, 273–275 (2003).
134. Gruber, N., Bates, N. R. & Keeling, C. D. Interannual variability in the North Atlantic carbon sink. *Science* **298**, 2374–2378 (2002).
135. Frölicher, T. L., Joos, F., Raible, C. C. & Sarmiento, J. L. Atmospheric CO_2 response to volcanic eruptions: the role of ENSO, season, and variability. *Glob. Biogeochem. Cycles* **27**, 239–251 (2013).
136. DeVries, T. Atmospheric CO_2 and sea surface temperature variability cannot explain recent decadal variability of the ocean CO_2 sink. *Geophys. Res. Lett.* **49**, 1–12 (2022).
137. Terhaar, J., Frölicher, T. L. & Joos, F. Observation-constrained estimates of the global ocean carbon sink from Earth system models. *Biogeosciences* **19**, 4431–4457 (2022).
138. Rogelj, J., McCollum, D. L., O'Neill, B. C. & Riahi, K. 2020 emissions levels required to limit warming to below 2°C. *Nat. Clim. Chang.* **3**, 405–412 (2012).
139. Keller, D. P. et al. The effects of carbon dioxide removal on the carbon cycle. *Curr. Clim. Chang. Rep.* **4**, 250–265 (2018).
140. Smith, P. et al. Biophysical and economic limits to negative CO_2 emissions. *Nat. Clim. Chang.* **6**, 42–50 (2016).
141. National Academies of Sciences. *A Research Strategy for Ocean-based Carbon Dioxide Removal and Sequestration* (National Academies Press, 2022).
142. Aricò, S. et al. *Integrated Ocean Carbon Research: A Summary of Ocean Carbon Research, and Vision of Coordinated Ocean Carbon Research and Observations for the Next Decade* Report No. 158 (IOC, 2021).
143. Gruber, N., Boyd, P. W., Frölicher, T. L. & Vogt, M. Biogeochemical extremes and compound events in the ocean. *Nature* **600**, 395–407 (2021).
144. Djeutchouang, L. M., Chang, N., Gregor, L., Vichi, M. & Monteiro, P. M. S. The sensitivity of pCO_2 reconstructions to sampling scales across a Southern Ocean sub-domain: a semi-idealized ocean sampling simulation approach. *Biogeosciences* **19**, 4171–4195 (2022).
145. Majkut, J. D. et al. An observing system simulation for Southern Ocean carbon dioxide uptake. *Philos. Trans. R. Soc. A Math. Phys. Eng. Sci.* **372**, 20130046–20130046 (2014).
146. Claustre, H., Johnson, K. S. & Takeshita, Y. Observing the global ocean with Biogeochemical-Argo. *Ann. Rev. Mar. Sci.* **12**, 23–48 (2020).
147. Gray, A. R. et al. Autonomous biogeochemical floats detect significant carbon dioxide outgassing in the high-latitude Southern Ocean. *Geophys. Res. Lett.* **45**, 9049–9057 (2018).
148. Bushinsky, S. M. et al. Reassessing Southern Ocean air–sea CO_2 flux estimates with the addition of biogeochemical float observations. *Glob. Biogeochem. Cycles* **33**, 1–19 (2019).
149. Verdy, A. & Mazloff, M. R. A data assimilating model for estimating Southern Ocean biogeochemistry. *J. Geophys. Res. Ocean.* **122**, 6968–6988 (2017).
150. Carroll, D. et al. Attribution of space–time variability in global-ocean dissolved inorganic carbon. *Glob. Biogeochem. Cycles* **36**, 1–24 (2022).
151. Bennington, V., Gloege, L. & McKinley, G. A. Variability in the global ocean carbon sink from 1959 to 2020 by correcting models with observations. *Geophys. Res. Lett.* **49**, e2022GL098632 (2022).
152. Lacroix, F., Ilyina, T. & Hartmann, J. Oceanic CO_2 outgassing and biological production hotspots induced by pre-industrial river loads of nutrients and carbon in a global modeling approach. *Biogeosciences* **17**, 55–88 (2020).
153. Kwon, E. Y. et al. Stable carbon isotopes suggest large terrestrial carbon inputs to the global ocean. *Glob. Biogeochem. Cycles* https://doi.org/10.1029/2020gb006684 (2021).
154. Joint Group of Experts on the Scientific Aspects of Marine Environmental Protection. High level review of a wide range of proposed marine geoengineering techniques. Report No. 98. *GESAMP.org* http://www.gesamp.org/publications/high-level-review-of-a-wide-range-of-proposed-marine-geoengineering-techniques (2019).
155. Dlugokencky, E. & Tans, P. Trends in atmospheric carbon dioxide. *National Oceanic & Atmospheric Administration; Global Monitoring Laboratory (NOAA/GML)* http://gml.noaa.gov/ccgg/trends/ (2022).
156. Gruber, N. & Sarmiento, J. L. in *THE SEA: Biological–Physical Interactions in the Oceans* Vol. 12 (eds Robinson, A. R., McCarthy, J. J. & Rothschild, B. J.) 337–399 (Wiley, 2002).
157. Kroeker, K. J. et al. Impacts of ocean acidification on marine organisms: quantifying sensitivities and interaction with warming. *Glob. Chang. Biol.* **19**, 1884–1896 (2013).
158. Landschützer, P., Gruber, N., Bakker, D. C. E., Stemmler, I. & Six, K. D. Strengthening seasonal marine CO_2 variations due to increasing atmospheric CO_2. *Nat. Clim. Chang.* **8**, 146–150 (2018).
159. Hauck, J. & Völker, C. Rising atmospheric CO_2 leads to large impact of biology on Southern Ocean CO_2 uptake via changes of the Revelle factor. *Geophys. Res. Lett.* **42**, 1459–1464 (2015).

Acknowledgements
N.G., J.D.M., L.G. and P.L. acknowledge support from the European Union's Horizon 2020 research and innovation programme under grant agreement No. 821003 (project 4C). N.G. also acknowledges support from the EU Horizon project no. 821001 (SO-CHIC). The work of D.C.E.B. was supported by the EU Horizon project no. 820989 (COMFORT). The work reflects only the authors' views; the European Commission and their executive agency are not responsible for any use that may be made of the information the work contains. G.A.M. acknowledges funding from the National Science Foundation (NSF) through LEAP STC (2019625) and OCE (1948624), the National Aeronautics and Space Administration (NASA) (80NSSC22K0150) and the National Oceanic and Atmospheric Administration (NOAA) (NA20OAR4310340). J.H. received funding from the Helmholtz Young Investigator Group Marine Carbon and Ecosystem Feedbacks in the Earth System (MarESys) (grant number VH-NG-1301). T.D. acknowledges support from NSF award OCE-1948955.

Author contributions
N.G. led the conceptual design and the implementation and also wrote the first draft. J.D.M. was responsible for the generation of Fig. 1 and Table 1. P.L. generated Fig. 2, L.G. generated Figs. 3 and 4, and N.G. drew Fig. 5. All authors contributed to the outline, discussed the content and conclusions and provided input to the manuscript during all drafting stages.

Competing interests
The authors declare no competing interests.

Additional information
Supplementary information The online version contains supplementary material available at https://doi.org/10.1038/s43017-022-00381-x.

Correspondence should be addressed to Nicolas Gruber.

Peer review information *Nature Reviews Earth & Environment* thanks K. Matsumoto and the other, anonymous, reviewer(s) for their contribution to the peer review of this work.